

The thermodynamics of computational copying in biochemical systems

Thomas E. Ouldridge,¹ Christopher C. Govern,² and Pieter Rein ten Wolde²

¹⁾Department of Mathematics, Imperial College London, London, SW7 2AZ, UK^{a)}

²⁾FOM Institute AMOLF, Science Park 104, 1098 XE Amsterdam, The Netherlands

Living cells use readout molecules to record the state of receptor proteins, similar to measurements or copies in typical computational devices. But is this analogy rigorous? Can cells be optimally efficient, and if not, why? We show that, as in computation, a canonical biochemical readout network generates correlations; extracting no work from these correlations sets a lower bound on dissipation. For general input, the biochemical network cannot reach this bound, even with arbitrarily slow reactions or weak thermodynamic driving. It faces an accuracy-dissipation trade-off that is qualitatively distinct from and worse than implied by the bound, and more complex steady-state copy processes cannot perform better. Nonetheless, the cost remains close to the thermodynamic bound unless accuracy is extremely high. Additionally, we show that biomolecular reactions could be used in thermodynamically optimal devices under exogenous manipulation of chemical fuels, suggesting an experimental system for testing computational thermodynamics.

PACS numbers: 87.10.Vg, 87.16.Xa, 87.18.Tt, 05.70.-a

If it were possible to perform many measurements using a single bit of memory without putting in work, Maxwell's Demon could use the information gained to violate the second law of thermodynamics and extract net work from an equilibrium system. Landauer's insight that computational processes require a physical instantiation and therefore have thermodynamic consequences^{1–3} is key to exorcising the Demon, and the survival of the second law has been demonstrated in a range of physical models^{2–4}. If, unlike Maxwell's thought experiment, the correlations generated by a measurement or copy are not used to perform work, the cycle increases the entropy of the universe (by at least $k \ln 2$ if the measurement is binary, perfectly accurate and has a 50/50 outcome)^{2,4}. Landauer and others have provided specific physical implementations of binary devices along with protocols that achieve the thermodynamic bound for measurement cycles^{2,3} or memory erasure protocols^{1,5–8}. Examples include magnetic systems^{1,2,8}, or single particles in pistons^{4,9–13}.

Do biomolecules perform measurement and copying within this computational paradigm? Many biological processes involve creating long-lived molecular copies of other molecules^{2,14,15}. Perhaps the most tantalising analogy is in the cellular sensing of external ligand concentrations. Following the seminal work of Berg and Purcell¹⁶, it has been shown that cells can reduce their sensing error by averaging a noisy receptor signal over time^{17–24}. Recent studies claim that cells implement time integration by dissipatively copying receptor states into the chemical modification states of readout molecules^{24–26}. Other authors have highlighted the necessity of dissipation in adaption^{27–29} and kinetic proofreading³⁰.

While it has been noted that there is a connection between the dissipation present in cellular copying and the

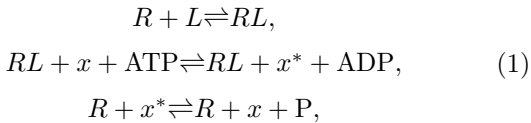
thermodynamics of computation^{24–26}, the nature of the connection remains nebulous. How do cellular protocols compare to the canonical copy protocols typically considered in the computational literature? Can cellular systems reach the fundamental thermodynamic limit on the accuracy and energetic cost of a measurement? If not, what is the underlying reason for the additional dissipation? Is it due to the nature of the biomolecular reactions, or due to the design of the signalling network? And if cellular systems cannot reach the fundamental limit, how does the trade-off between energy and precision differ from the ideal case? To answer these questions, it is necessary to construct a rigorous mapping between cellular processes and computational copying. Understanding the connection between the thermodynamics of computation and the thermodynamics of biological processes^{24,25,27,30–35} at a mechanistic level would enable translating quantitative, not just qualitative, results from the literature on computation.

Here, we map a canonical push-pull signalling motif to a computational copy device at the level of the master equation. The uncontrolled loss of correlations generated between receptors and readouts (rather than the widely discussed costs of “erasure”) sets a lower bound on the dissipation. We show that the push-pull network cannot converge on this fundamental limit for a general input signal, regardless of its parameters, and we prove that more complex biochemical networks involving multiple steps or parallel pathways cannot perform any better. Remarkably, however, biochemical networks can operate close to the lower bound at moderate-to-high accuracy, even at a high rate of copying. Further, cellular networks are naturally adaptive, dissipating less when the sampling challenge is reduced. Finally we show that an artificial copy device based on biochemical reactions can achieve the thermodynamic bound with exogenous manipulation of fuel concentrations, providing an alternative platform for investigating the thermodynamics of computation.

^{a)}Electronic mail: t.ouldridge@imperial.ac.uk

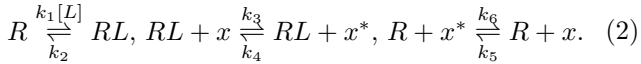
I. RESULTS

Mapping a cellular biochemical network to a copy process. We consider bi-functional kinase systems, which are common in bacteria³⁶. The bi-functional kinase either tends to phosphorylate or dephosphorylate a readout x , depending on the ligand-binding state of the receptor to which the kinase is coupled (Fig. 1). If the receptor R is bound to ligand L , then the bi-functional kinase acts as a kinase, catalyzing phosphorylation and dephosphorylation reactions that are both coupled to ATP hydrolysis. If the receptor is not bound to ligand, then the bi-functional kinase acts as a phosphatase, catalyzing phosphorylation and dephosphorylation reactions that are uncoupled from ATP hydrolysis. Such a system can be described by the following reactions



where the kinase/phosphatase activity is coarse-grained into the ligand-binding state of the receptor. Here x and x^* represent unphosphorylated and phosphorylated readout states, respectively. In this manuscript we will use R , RL , x and x^* to represent both molecular species and the number of molecules of that type, depending on context.

For simplicity, we take $[L]$ to be constant, and assume the system is maintained in a non-equilibrium steady state: $[ADP]$, $[ATP]$ and $[P]$ are fixed. We treat phosphorylation and dephosphorylation as instantaneous second-order reactions. Thus



The master equation for this system, and the chemical kinetics approximation, are provided in Supplementary Discussion 1. We emphasize that the reactions within each equation are the microscopic reverses of each other, while the reactions of the second and third equations correspond to distinct reaction paths. This yields a thermodynamically consistent model.

Qualitatively, this circuit performs copies (or measurements) in the following way. As spontaneous phosphorylation and dephosphorylation in the absence of the bi-functional kinase occur at a low rate which we take to be zero, the two chemical modification states of the readout are analogous to two stable states of a memory bit separated by a large barrier, as widely considered in the computational literature^{2,3,14}. There are, however, two separate paths between the two wells, via exchange of phosphate with ATP and via exchange of phosphate with the cytosol. Moreover, the ATP-independent (de)phosphorylation reaction has a high yield of x in equilibrium, whereas the ATP-coupled reaction has an intrinsically high yield of x^* . The resultant extended free-energy landscape for a single readout that explicitly considers ATP turnover is illustrated in Fig. 1B.

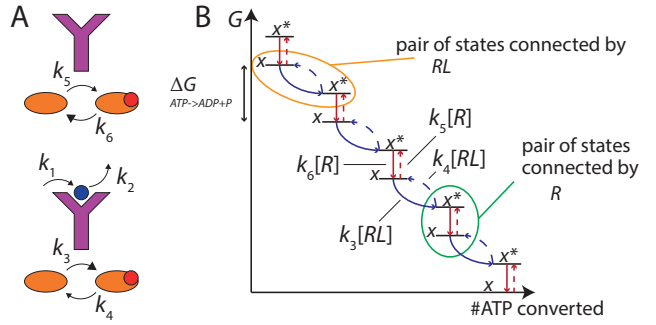


FIG. 1. A canonical signaling network. (A) The signaling network utilizes a receptor that acts as a bifunctional kinase/phosphatase: when bound to ligand, it catalyses the activation of the downstream readout; when unbound, it catalyzes the deactivation of the downstream readout. Free-energy dissipation due to the use of fuel, coarse-grained from this representation, drives the reactions. (B) Schematic free-energy landscape of a single readout molecule in the biochemical network. We plot the free energy G as a function of the number of ATP molecules that are converted into ADP molecules, for the two states x and x^* . Thermodynamically favourable transitions are shown with solid arrows, and unfavourable transitions with dashed arrows. The presence of catalysts R and RL makes these transitions faster, and thereby push the system towards x or x^* , but the overall thermodynamic drive is fixed for both reactions.

presence of RL lowers the barrier between pairs of states connected by ATP turnover, whereas the presence of R lowers the barrier between states not connected by ATP turnover. In this way, the receptor will, depending on its ligand-binding state, push readouts towards either x or x^* , which can then be thought of as copying the state of the receptor into the chemical modification state of the readout^{24,25}. We will now make this analogy concrete, allowing a quantitative analysis of biochemical copying.

Since each readout molecule provides a stable memory of the receptor state, the readout molecules collectively encode the receptor history. This enables time integration of the receptor signal and hence enhanced accuracy of concentration estimates.^{16,24,25} We are not concerned, however, with the precision of sensing a constant concentration^{16,17,24,25,37}, nor with the “learning rate” between the ligand concentration and the network, which is important when changes in external concentrations are more rapid^{38–40}. Rather, we are interested in whether the readout reaction can be rigorously described in terms of a copy process, and if so, how this cellular protocol compares to optimal quasistatic computational protocols involving the manipulation of energy landscapes that are common in the literature^{2,3,14}.

The biochemical network as a copy process. Let us consider the dynamics necessary for the biochemical network to truly perform stochastic copying. Each readout molecule should perform a copy of any one ligand-bound receptor at a rate k_{copy}^{RL} , and any one unbound receptor

at a rate k_{copy}^R . These copies are performed with accuracies s_{RL} and s_R respectively, and the result of the copy is independent of the prior state of the readout. Thus a copy of RL (R) returns x^* (x) with probability s_{RL} (s_R). At the level of the master equation, old copies in state x should be converted into new copies in state x^* at a rate

$$\sigma_{x \rightarrow x^*} = (N_{RL}k_{\text{copy}}^{RL}s_{RL} + N_Rk_{\text{copy}}^R(1 - s_R))x, \quad (3)$$

in which N_R and N_{RL} are numbers of receptors in each state, and x^* should be converted into x at a rate

$$\sigma_{x^* \rightarrow x} = (N_{RL}k_{\text{copy}}^{RL}(1 - s_{RL}) + N_Rk_{\text{copy}}^R s_R)x^*. \quad (4)$$

Returning to our actual biochemical network, Eq. 2 specifies the dynamics of x and x^* . The transitions occur with rates

$$\begin{aligned} \sigma_{x \rightarrow x^*} &= (k_3[RL] + k_5[R])x, \\ \sigma_{x^* \rightarrow x} &= (k_4[RL] + k_6[R])x^*. \end{aligned} \quad (5)$$

Comparing Eqs. 3-5, we see that the biochemical network is equivalent to a stochastic copy process with

$$k_{\text{copy}}^{RL} = (k_3 + k_4)/V, \quad k_{\text{copy}}^R = (k_5 + k_6)/V, \quad (6)$$

in which V is the volume of the system and the copy accuracies are

$$s_{RL} = k_3/(k_3 + k_4), \quad s_R = k_6/(k_5 + k_6). \quad (7)$$

Copies are therefore made at a rate $(k_{\text{copy}}^{RL}N_{RL} + k_{\text{copy}}^RN_R)x_T$, which gives an average copy rate

$$\dot{n}_{\text{copy}} = x_T((k_3 + k_4)\langle[RL]\rangle + (k_6 + k_5)\langle[R]\rangle), \quad (8)$$

in which x_T is the total number of readouts. Thus the biochemical network can be directly mapped to a stochastic copying process.

Energetic cost per copy cycle. In the non-equilibrium steady state, the average dissipation rate of chemical free energy (\dot{w}_{chem}) is

$$\dot{w}_{\text{chem}} = -\dot{n}_{\text{flux}}(\Delta\mu_1 + \Delta\mu_2) = \dot{n}_{\text{flux}}kT \ln\left(\frac{k_3k_6}{k_4k_5}\right), \quad (9)$$

where \dot{n}_{flux} is the average current of readout molecules around the phosphorylation/dephosphorylation loop; $\Delta\mu_1 = \mu_{\text{ADP}} - \mu_{\text{ATP}}$ and $\Delta\mu_2 = \mu_P$. The sum $-(\Delta\mu_1 + \Delta\mu_2)$ is therefore the total free energy dissipated when a readout goes around this cycle once.

To proceed, we introduce the following averages:

$$p = \frac{\langle RL \rangle}{R_T} = \frac{k_1[L]}{k_2 + k_1[L]}, \quad f = \frac{\langle [x^*] \rangle}{\langle [x_T] \rangle}, \quad (10)$$

with R_T the total number of receptors. In the mean-field limit, \dot{n}_{flux} follows from Eq. 2 as

$$\dot{n}_{\text{flux}} = \langle k_3RL[x] - k_4RL[x^*] \rangle = (k_3(1 - f) - k_4f)p[x_T]R_T. \quad (11)$$

Furthermore, the fraction of phosphorylated readout f is

$$f = \frac{k_3p + k_5(1 - p)}{(k_3 + k_4)p + (k_5 + k_6)(1 - p)}, \quad (12)$$

giving

$$\dot{w}_{\text{chem}} = \frac{(k_3k_6 - k_4k_5)p(1 - p)[x_T]R_T}{(k_3 + k_4)p + (k_5 + k_6)(1 - p)}kT \ln\left(\frac{k_3k_6}{k_4k_5}\right). \quad (13)$$

For the full calculation, we refer to Supplementary Discussion 1. The mean field approach holds in the limit of many receptors, or when the receptor dynamics is fast. If these conditions are not met, readouts perform copies of receptor states that are correlated with the current readout state. Detailed analysis of this regime is beyond the scope of this work, but a brief discussion is provided in Supplementary Discussion 1.

Given the rate of copying (Eq. 8) and the rate at which chemical work is done (Eq. 13), we are now in a position to calculate the chemical work done per copy cycle:

$$\frac{w_{\text{chem}}}{n_{\text{copy}}} = \frac{(k_3k_6 - k_4k_5)p(1 - p)}{((k_3 + k_4)p + (k_5 + k_6)(1 - p))^2}kT \ln\left(\frac{k_3k_6}{k_4k_5}\right). \quad (14)$$

This result can be simplified by noting that the probability a copy is made of RL is not p , but rather

$$p' = p \frac{k_3 + k_4}{(k_3 + k_4)p + (k_5 + k_6)(1 - p)}. \quad (15)$$

Indeed, if $k_3 + k_4 > k_5 + k_6$, a ligand-bound receptor is more frequently copied than an unbound receptor molecule. This expression allows us to rewrite Eq. 14 as

$$\frac{w_{\text{chem}}}{n_{\text{copy}}} = (s_R + s_{RL} - 1)p'(1 - p')kT \ln\left(\frac{k_3k_6}{k_4k_5}\right). \quad (16)$$

The quantity $kT \ln \frac{k_3k_6}{k_4k_5}$ has dimensions of energy and is equal to the chemical work done during a single phosphorylation/dephosphorylation cycle. We can split it into an energy related to the accuracy of copying RL , $E_{s_{RL}} = kT \ln(k_3/k_4) = kT \ln(s_{RL}/(1 - s_{RL}))$, and an energy related to the accuracy of copying R , $E_{s_R} = kT \ln(k_6/k_5) = kT \ln(s_R/(1 - s_R))$. In these terms,

$$\frac{w_{\text{chem}}}{n_{\text{copy}}} = (s_R + s_{RL} - 1)p'(1 - p')(E_{s_R} + E_{s_{RL}}). \quad (17)$$

Inverting the sign of E_{s_R} and $E_{s_{RL}}$ corresponds to a mirror-image encoding, in which RL is copied to x and R to x^* . Low accuracy corresponds to $E_{s_R}, E_{s_{RL}} \rightarrow 0$, when $s_R \approx \frac{1}{2}(1 + E_{s_R}/2kT)$, and $s_{RL} \approx \frac{1}{2}(1 + E_{s_{RL}}/2kT)$. In the symmetric case of $E_{s_R} = E_{s_{RL}} = -\Delta\mu/2$, the accuracy of copies is $s_R = s_{RL} = \frac{1}{2}(1 - \Delta\mu/4kT)$. A similar analysis, with an equivalent outcome, is performed in Supplementary Discussion 2 for a related system in which receptors act only as kinases.

Optimal devices and the thermodynamic bound. The biochemical network has the dynamics of a process in

which readouts randomly perform copies of receptors. It is also fundamentally dissipative – does the fact that it is a copy process set a practically relevant thermodynamic bound on this dissipation?

We can calculate the minimal thermodynamic cost of the random computational copy process that is equivalent to our network motif. In each copy operation, a memory bit (in a state x^* with probability $f(s_{RL}, s_R, p')$) is exposed to data (in state RL with probability p') - the final result is a memory bit in state x^* with probability s_{RL} or $1 - s_R$, conditional on the data. Mutual information I is then generated between the data and the memory.

After the copy step, the data (receptor) and memory (readout) are decoupled without loss of information. This means that they remain correlated, even though there is no direct physical interaction between the data and memory anymore. The fact that they remain correlated in the absence of direct interactions implies that the system is out of equilibrium: the free energy stored in the correlations is kTI .^{4,15,41} Making computational copies thus amounts to storing free energy in mutual information, and if this information is not used to extract work (as done by an efficient Maxwell Demon) but simply lost in an uncontrolled fashion during a subsequent measurement, then the process is irreversible and the information lost sets a lower bound on dissipation. In the random copy process, the stored information is overwritten without being used to extract work, and hence kTI sets a lower bound on the dissipation for the entire cyclic copy operation, as noted in Ref. 4. A copying device and a set of quasistatic protocols that can achieve this bound for various input data are given in Supplementary Fig. 1 and analysed in Supplementary Discussion 3.

The biochemical network considered here has the dynamics of a random copy process, and, indeed, work is not extracted from the information generated. Thus its dissipation is constrained by the mutual information generated in the stochastic copy process:

$$\frac{w_{\text{chem}}}{kTn_{\text{copy}}} \geq I = p's_{RL} \ln \left(\frac{s_{RL}}{f} \right) + p'(1 - s_{RL}) \ln \left(\frac{1 - s_{RL}}{1 - f} \right) + (1 - p')s_R \ln \left(\frac{s_R}{1 - f} \right) + (1 - p')((1 - s_R) \ln \left(\frac{1 - s_R}{f} \right)). \quad (18)$$

This bound implies an efficiency $\eta = (kTI)/(w/n_{\text{copy}}) \leq 1$, which is unity for an optimal protocol.

The readout molecule states are persistent – the ligand-binding state of the receptor is remembered even after detaching, thus enabling time integration^{24,26}. Systems that do not make persistent copies, including passive readouts²⁶, the receptors themselves and also some more complicated networks²⁸, are not bound by the same limit. Previous work has linked energy dissipation in similar systems to the erasure of the memory^{24,25}, that is the resetting of the memory bit to a well-defined state. As shown by Landauer, this erasure does lead to the transfer of heat from the system to the surroundings. Resetting a bit, however, is not intrinsically thermodynamically

irreversible^{2,3,10,13,42} – indeed, Landauer's calculation of the minimal heat transfer applies to a thermodynamically reversible erasure step. It is therefore the uncontrolled loss of correlations (the failure to extract work from them) rather than erasure itself, which is the origin of the thermodynamic irreversibility of a copy cycle. It is also this failure that sets the fundamental thermodynamic lower bound on the work to perform copy cycles. In fact, erasure is not even necessary in an optimal copy cycle, which leaves open the possibility that the biochemical network, which actually contains no explicit erasure, could achieve the lower bound. For more details, see Supplementary Discussion 3.

Trade-off between dissipation and error. The bound in Eq. 18 holds for all choices of s_{RL} , s_R and p' . But how close does the biochemical network come to this bound, and can it be reached in certain conditions? Our concrete mapping allows us to examine these questions.

Initially, we consider the simplest case of equal accuracy ($s_R = s_{RL} = s$). The dissipation per copy cycle for the biochemical network (Eq. 17) then reduces to

$$\frac{w_{\text{chem}}}{n_{\text{copy}}} = 2E_s(2s - 1)p'(1 - p'), \quad (19)$$

with $E_s = E_{s_{RL}} = E_{s_R}$. The chemical work per copy cycle, $w_{\text{chem}}/n_{\text{copy}}$, is plotted against p' in Fig. 2 A-B for two values of s (red dashed lines). We also indicate behaviour forbidden by the thermodynamic bound of Eq. 18 (grey region). In Fig. 2 (C), we fix $p' = 0.5$ and plot the cost per copy cycle against s for the biochemical network (red dashed line) and an optimal system that saturates the bound (solid blue line).

Both the cost of biochemical network and the thermodynamic bound drop as the required accuracy is decreased. The irreversible loss of information bounds the work, and lower accuracy implies less information to be lost. It is clear from Fig. 2 (C), however, that the two systems have a very different tradeoff between dissipation and accuracy. The required free-energy input for the biochemical case diverges as $s \rightarrow 1$ ($w_{\text{chem}}/n_{\text{copy}} \approx -2p'(1 - p')kT \ln(1 - s)$), whereas the dissipated work remains finite in an optimal system. It is clear that a cell will have to sacrifice some accuracy for the sake of efficiency. Even in the limit of low accuracy ($s \rightarrow \frac{1}{2}$) and at $p' = 0.5$, the biochemical network is twice as costly as the bound ($\eta \rightarrow \frac{1}{2}$ from above). Expanding Eqs. 18 and 19 for $s \rightarrow \frac{1}{2}$ gives $w_{\text{chem}}/n_{\text{copy}} \approx 4kT(s - \frac{1}{2})^2$ for the biochemical network and $w_{\text{chem}}/n_{\text{copy}} \approx 2kT(s - \frac{1}{2})^2$ for the optimal device and protocol.

The fundamental difference between the biochemical network and an optimal protocol is illustrated in Fig. 3. An optimal protocol requires reversible quasistatic manipulation of energy levels. In the biochemical network, however, the energy levels are fixed. Only the barrier heights and hence the reaction rates are modulated, due to the presence or R or RL . As a consequence, biasing transitions is more costly in the biochemical system.

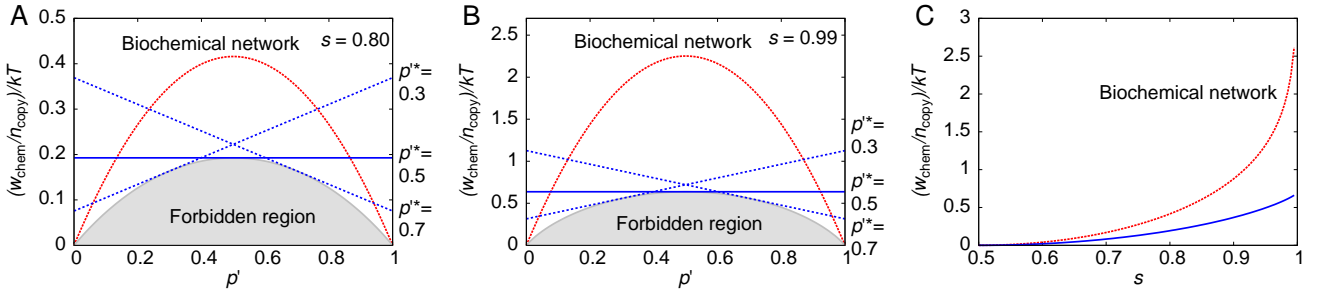


FIG. 2. Trade-off between dissipation and accuracy in copying. The (chemical) work per copy cycle for different probabilities p' of attempting to copy RL is plotted at two different values of the measurement accuracy: (A) $s = 0.80$; and (B) $s = 0.99$. Note that $p' = p$, the probability that a receptor is in state RL , if $k_3 + k_4 = k_5 + k_6$ when the sampling rate for the two receptor states is the same. The biochemical implementation (red line) does not achieve the lower bound for a measuring device, which is the border of the shaded region. The blue lines correspond to quasistatic protocols for the device in Supplementary Fig. 1 (see Supplementary Discussion 3) and are optimal for a specific value of p' , p^* , at the given values of s . (C) Dissipation per copy cycle at $p' = 0.5$ as a function of s for the biochemical network (dashed red line) and a system that saturates the bound (solid blue line). The solid blue line ($p^* = 0.5$) saturates at $kT \ln 2$ for perfect accuracy ($s = 1$) and the cost of the canonical biochemical motif diverges.

This difference is particularly intuitive in the limits of low and high copy accuracy for $p' = 0.5$. For the biochemical network, the difference between the fraction of correct copies s , and the fraction of incorrect copies $1 - s$, is $2(s - \frac{1}{2})$. For $p' = 0.5$, in only half of these cases does a reaction occur and so the net number of reactions in the intended direction is $s - \frac{1}{2}$ per copy cycle. Each of these net reactions has a cost given by the driving free energy, $E_s \approx 4(s - \frac{1}{2})kT$, giving an overall cost per copy cycle of $w_{\text{chem}}/n_{\text{copy}} \approx 4kT(s - \frac{1}{2})^2$. For an optimal quasistatic protocol, a similar argument can be constructed (see Supplementary Discussion 3), but the average energy offset between the states at which a transition occurs is less than the final offset required by the accuracy, E_s . In the limit of $E_s \rightarrow 0$, we obtain an average cost of $E_s/2$, rather than E_s as for the biochemical network.

In the limit of high accuracy, $s \rightarrow 1$ and $E_s \rightarrow \infty$, a similar analysis shows why the biochemical network is much less efficient than an optimal quasistatic protocol. The cost of each transition continues to grow linearly with E_s in the biochemical network, explaining the divergence of chemical work with s . In an optimal protocol, however, the work saturates when $E_s \gg kT$. In this case, the energy difference between the two states is raised quasistatically to E_s . Therefore at each moment in time, the bit is in equilibrium. As E is raised, the probability that the bit is in the high energy state decreases, until it rapidly becomes negligible when $E > kT$ and the higher energy state can be raised further without any additional cost.

As is evident from Figs. 2 (A,B), the cost of both an optimal system and the biochemical network decrease as we move away from $p' = 0.5$ at fixed s . Fixed accuracy measurement results in less information if the data itself has low entropy, explaining the reduction in the bound. For the biochemical network, if the readout is exposed more often to one receptor state, it is more likely to be in the appropriate output state prior to a copy. Hence,

fewer transitions are needed and less dissipation occurs. For an alternative network in which receptors only function as kinases, this automatic compensation only occurs at low p (see Supplementary Discussion 2).

In Supplementary Fig. 2 we plot the efficiency η as a function of $p' \neq 0.5$ and $s = s_R = s_{RL}$; η is actually highest for $p' \rightarrow 0$ or 1 (when $\eta \rightarrow \frac{1}{2}$ from below for all s), and lowest at $p' = \frac{1}{2}$. This intrinsic adaption is fundamentally different from the behaviour of typical computational devices such as that in Supplementary Fig. 1. For these devices the protocol must be adjusted as p' is varied, via a parameter related to decorrelation, to make the system optima (see Supplementary Discussion 3 for further details). Figs. 2 (A,B) show, with blue lines, the work per copy of three fixed protocols for the device in Supplementary Fig. 1. These protocols are optimal for $p^* = 0.3, 0.5$ and 0.7 , respectively, and the lines are tangent to the forbidden region at these values of p' , but above it elsewhere. It is not clear whether an alternative protocol exists that reaches the bound for all p' without any adjustment of a parameter, though it seems unlikely.

None of the “optimal” protocols for the device in Supplementary Fig. 1 perform better than the biochemical network for all values of p' . Given knowledge of p' , a system using quasistatic manipulations could reach the limiting efficiency of a copying device that does not extract work from the correlations it generates. In our cellular context, however, p' is the quantity that the system is trying to measure (rather than the state of individual receptors given a known p'). The best that could be done, therefore, would be to pick a particular protocol, and update it as more information became available. Clearly, however, implementing this behaviour in an autonomous device would require substantial additional complexity.

We have shown that the biochemical network cannot reach the fundamental limit of efficiency for $s_R = s_{RL}$, regardless of the system parameters. Neither reducing

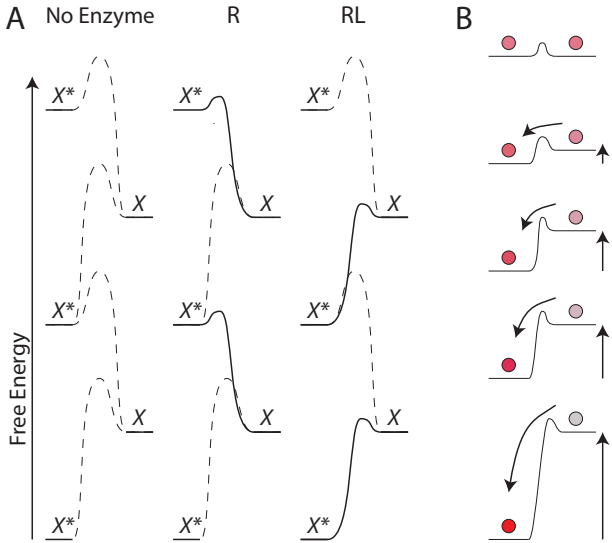


FIG. 3. Schematic comparison between the (free-) energy landscapes of the biochemical network (A) and a thermodynamically optimal protocol (B). In (A), a ladder of states exists, with successive rungs related by the turnover of a single ATP (implicit in this figure, explicit in Fig. 1). In the absence of an enzyme, all transitions are slow (indicated by the dashed free-energy barrier connecting the states). In the presence of R , half of the transitions are catalysed and can occur rapidly (solid lines); when exposed to RL , the alternative transitions are rapid. The heights of the rungs, however, are fixed, meaning that all transitions involve a fixed amount of chemical work equal to the offset. By contrast, for the optimal protocol in (B), switching between states is driven by slowly destabilizing one state with respect to the other, so that the majority of transitions have already occurred before the offset approaches its limiting value.

the reaction rates nor the thermodynamic driving permits $\eta > 1/2$. It is sometimes assumed that systems under steady-state forcing are effectively quasistatic or reversible in the limit of this forcing being weak²⁵ – clearly that is not the case here. For $s_R \neq s_{RL}$, it is possible to obtain an efficiency $\eta > 1/2$, and η can even approach unity for extreme values of p' , s_R and s_{RL} (see Supplementary Fig. 3 and Supplementary Discussion 4). Nonetheless, it remains true that η cannot converge on unity for general p' , regardless of how s_R and s_{RL} are varied. The biochemical network is more dissipative than an optimal process, because operating at a constant thermodynamic driving force leads to more energetically expensive transitions than slowly manipulating energy levels.

Thus far we have emphasized differences between the thermodynamic bound and the cost of the biochemical protocol. It is remarkable, however, that the biochemical network comes so close to the lower bound, even at fairly high accuracies. Reaching 99% accuracy for $p' = 0.5$ requires less than four times the dissipation of the lower bound, and η is even higher for $p' \neq 0.5$. Further, this efficiency can be achieved at an arbitrarily high rate of copying – the absolute rates do not enter the expression

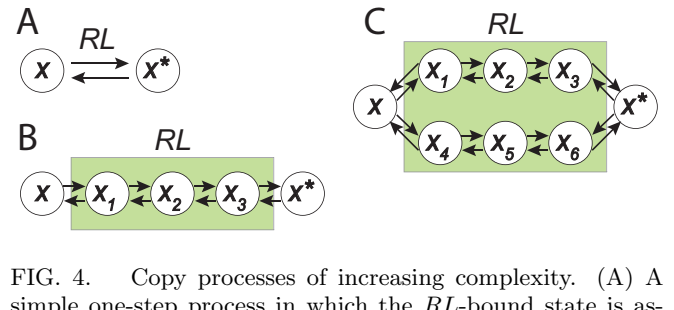


FIG. 4. Copy processes of increasing complexity. (A) A simple one-step process in which the RL -bound state is assumed short-lived. (B) A tightly-coupled process in which the readout passes through multiple states whilst bound to the receptor, but only one pathway is possible. (C) A more general process in which multiple pathways between x and x^* exist. Each different path *could* be associated with different entropy increases in the environment.

in Eq. 19. Through our quantitative mapping, we have shown that a physically reasonable model system operating autonomously at an arbitrary rate and with a high copying accuracy comes close to the fundamental thermodynamic limit on the cost of a copy process.

One-step copy processes are maximally efficient for the biochemical network. The push-pull network considered so far is a one-step copy process, with the conversion between the phosphorylation states occurring via a single instantaneous transition. We now show that more complex processes, involving multiple steps or pathways, cannot improve the trade-off between energy and precision in autonomous, steady-state systems driven directly by an out-of equilibrium chemical fuel. We again consider Markov process with discrete states, but we now allow for multiple states and multiple parallel pathways between x and x^* (see Fig. 4). We explicitly consider the interconversion of x and x^* by RL ; an equivalent argument holds for reactions mediated by R . The autonomous requirement prohibits external control and implies that transition rates are fixed.

In the simple one-step process, the accuracy of copying RL is $s_{RL} = k_3/(k_3+k_4)$. In a more general process, however, transitions between x and x^* are not instantaneous and hence cannot be described with rate constants. The natural generalisation is to consider the flux ϕ from x to x^* and vice versa, which is defined as the rate at which trajectories leave x and subsequently reach x^* before returning to x .⁴³ The fluxes determine the copy accuracy in the same way as the rate constants for the one-step process, since they represent the rate receptors initiate correct and incorrect transitions between x and x^* .

Consider the accuracy of copying RL , $s_{RL} = \phi_3/(\phi_3 + \phi_4) = 1/(1 + \phi_4/\phi_3)$, which depends solely on ϕ_3/ϕ_4 . We define the set of paths \mathcal{S} that start by leaving x and reach x^* via an interaction with RL without returning to x . The entropy change in the environment $\Delta S_{\text{env}}[z(t)]$ due to each of these individual trajectories $z(t)$ is related to the probability of observing the forward pathway, and its

reverse $\tilde{z}(t)$:^{44–46}

$$\Delta S_{\text{env}}[z(t)] = k \ln \left(\frac{p[z(t)|z(0)=x]}{p[\tilde{z}(t)|\tilde{z}(0)=x^*]} \right) - \Delta S_{\text{int}}. \quad (20)$$

Here ΔS_{int} is an intrinsic entropy difference between macrostates x and x^* that arises because discrete biochemical states contain multiple microstates. It is a property of the states x and x^* , rather than the transitions, and will eventually cancel out in our analysis. We can then divide \mathcal{S} into subsets \mathcal{S}_i according to $\Delta S_{\text{env}}[z(t)]$; all paths within \mathcal{S}_i generate the same entropy in the environment, ΔS_{env}^i . Conceptually, different subsets might correspond to pathways that consume different amounts of ATP. A simple one-step pathway, as considered hitherto, is a special case of a system with a single \mathcal{S}_i .

The probability of observing any pathway within \mathcal{S}_i given an initial state $z = x$ is

$$P(\mathcal{S}_i|x) = \sum_{z(t) \in \mathcal{S}_i} p(z(t)|z(0)=x). \quad (21)$$

Similarly, $P(\mathcal{S}_{-i}|x^*) = \sum_{z(t) \in \mathcal{S}_{-i}} p(\tilde{z}(t)|\tilde{z}(0)=x^*)$ is the probability of observing a reverse of a pathway in \mathcal{S}_i given an initial state x^* . By design, $\Delta S_{\text{env}}^i + \Delta S_{\text{int}} = k \ln(P(\mathcal{S}_i|x)/P(\mathcal{S}_{-i}|x^*))$. Further, the ratio of forwards to backwards fluxes is given by

$$\frac{\phi_3}{\phi_4} = \frac{\sum_i P(\mathcal{S}_i|x)}{\sum_i P(\mathcal{S}_{-i}|x^*)}. \quad (22)$$

An immediate consequence is that in systems with only one subset of \mathcal{S} , in which all $\Delta S_{\text{env}} = \Delta S_{\text{env}}^{\text{tight}}$ associated with a transition are the same, the ratio of forwards to backwards fluxes is fixed by

$$k \ln \left(\frac{\phi_3}{\phi_4} \right) = \Delta S_{\text{env}}^{\text{tight}} + \Delta S_{\text{int}}. \quad (23)$$

Such a process is “tightly coupled”; in our framework, being tightly coupled implies that each transition x to x^* is associated with the breakdown of the same number of ATP molecules. Regardless of the number of intermediate steps or possible pathways in a tightly-coupled process between x and x^* , the copy accuracy is unambiguously determined by the entropy change in the environment. Thus all tightly-coupled process with the same accuracy are associated with the same dissipation. Since the one-step process we have considered hitherto is tightly-coupled, all tightly-coupled processes have the same accuracy/efficiency trade-off as we have derived.

It is also possible to consider processes that are not tightly-coupled, with multiple subsets \mathcal{S}_i . In this case, the average entropy deposition per $x \rightarrow x^*$ transition is given by

$$\Delta S_{\text{env}}^{\text{multi}} = k \sum_i \frac{P^{\text{m}}(\mathcal{S}_i|x)}{\sum_j P^{\text{m}}(\mathcal{S}_j|x)} \ln \left(\frac{P^{\text{m}}(\mathcal{S}_i|x)}{P^{\text{m}}(\mathcal{S}_{-i}|x^*)} \right) - \Delta S_{\text{int}}, \quad (24)$$

where we used the “m” superscript to denote probabilities for this specific multi-subset system. The accuracy of this process is still determined by Eq. 22: $\phi_3^{\text{multi}}/\phi_4^{\text{multi}} = \sum_i P^{\text{m}}(\mathcal{S}_i|x)/P^{\text{m}}(\mathcal{S}_{-i}|x^*)$. We can compare this multi-subset process to a tightly-coupled process with the same accuracy: $\phi_3^{\text{tight}}/\phi_4^{\text{tight}} = \phi_3^{\text{multi}}/\phi_4^{\text{multi}}$. The key point is that since entropy generation and accuracy are unambiguously related for a tightly-coupled process (Eq. 23), any tightly-coupled process between x and x^* with the same accuracy as the multi-subset generates

$$\Delta S_{\text{env}}^{\text{tight}} + \Delta S_{\text{int}} = k \ln \frac{\phi_3^{\text{multi}}}{\phi_4^{\text{multi}}} = k \ln \frac{\sum_i P^{\text{m}}(\mathcal{S}_i|x)}{\sum_i P^{\text{m}}(\mathcal{S}_{-i}|x^*)}. \quad (25)$$

Combining Eqns. 24 and 25 thus yields

$$\Delta S_{\text{env}}^{\text{multi}} - \Delta S_{\text{env}}^{\text{tight}} = \sum_i P_N^{\text{m}}(\mathcal{S}_i|x) \ln \left(\frac{P_N^{\text{m}}(\mathcal{S}_i|x)}{P_N^{\text{m}}(\mathcal{S}_{-i}|x^*)} \right), \quad (26)$$

where the subscript N indicates normalization: $P_N^{\text{m}}(\mathcal{S}_i|x) = P^{\text{m}}(\mathcal{S}_i|x)/\sum_j P^{\text{m}}(\mathcal{S}_j|x)$, and $P_N^{\text{m}}(\mathcal{S}_{-i}|x^*)$ is defined equivalently. Eq. 26 is a Kullback-Leibler divergence between the families of paths taken by forwards and backwards transitions in the multi-subset process, and is therefore necessarily non-negative. Thus

$$\Delta S_{\text{env}}^{\text{multi}} - \Delta S_{\text{env}}^{\text{tight}} \geq 0. \quad (27)$$

Similarly, paths that begin and end in x or x^* deposit no entropy for a tightly coupled process, whereas the entropy deposition of these paths is non-negative in general. For a system operating in steady state, increased entropy deposited into the environment implies less efficiency. Therefore no process of a given copy accuracy is more efficient than a tightly-coupled one. The limits derived for a one-step process, a special case of a tightly-coupled process are therefore general.

Our derivation is related to the proof that the estimate of dissipation obtained from the irreversibility of a coarse-grained trajectory gives a lower bound on the true entropy generation.^{47,48} The results are fundamentally distinct, however. We could consider coarse-graining a complex copy process so that all states were now x or x^* . However, the result would not be a simple one-step process with the same accuracy and lower dissipation; the dynamics would be non-Markovian and reflect the underlying complex process. To state that a true one-step process could reproduce the accuracy at the same cost as estimated from the coarse-grained description would be to assume the conjecture that is to be proven.

Biochemical implementation of an optimal device and protocol. We have argued that no cellular biochemical network, operating autonomously and directly powered by a non-equilibrium fuel supply, can reach the thermodynamic bound on efficiency for general input data. We now consider whether this is a fundamental property of biochemical reactions, or whether biomolecules could in principle act as thermodynamically optimal bits.

There are two principal differences between cellular biochemical network and optimal systems such as that in Fig. 3 and Supplementary Fig. 1^{2,3,14}. Firstly, cellular networks operates continuously, rather than taking a series of discrete measurements with external clocking. Secondly, as emphasized above, they involve no manipulation of energy levels.

Concerning the first difference, in Supplementary Discussion 5 we show that a clocked analogue of the cellular push-pull motif (illustrated in Supplementary Fig. 4) gives a work per copy identical to the continuous case. This is because, despite being operated in a clocked fashion, the device still out of equilibrium and functions at constant chemical potential of fuel molecules. The fact that cellular networks operate in a stochastic continuous manner rather than a clock-like fashion is not the fundamental reason why they cannot reach the bound on the energy cost of a copy operation.

Functioning out-of-equilibrium is necessary for a device operating at constant chemical potential of fuel; if the reactions were in equilibrium, the receptor (which is a catalyst) could not influence the yield of x/x^* . We now show that a system driven by quasistatic manipulation of ATP, ADP and P concentrations could reach the thermodynamic bound. To operate in the quasistatic limit, RL and R must be long-lived; in practice, constitutively active kinases and phosphatases could be used.

We consider a device and measurement cycle as illustrated schematically in Fig. 5. The key ingredients are the possibility of manipulating the concentrations of ATP, ADP and P in the vicinity of the readout, and the ability to bring the readout into or out of close proximity with receptors. We consider the same receptor/readout reactions as in Eq. 1, and now define the free energy changes of reaction ΔG_p for the phosphorylation of x by RL and ΔG_d for the dephosphorylation of x^* by R . These quantities are given by

$$\begin{aligned}\Delta G_p &= \mu_{ADP} - \mu_{ATP} + \Delta G_{x/x^*}, \\ \Delta G_d &= \mu_P - \Delta G_{x/x^*},\end{aligned}\quad (28)$$

in which $\Delta G_{x/x^*}$ quantifies the intrinsic stability of x and x^* (assumed to be independent of the chemical potentials of ATP, ADP and P⁴⁵). The reactions can thus be manipulated by controlling μ_{ATP} , μ_{ADP} and μ_P , for example by coupling of the system to a series of reservoirs (Fig. 5 (B)). We outline an optimal cycle below, and calculate the chemical work done on the readout subsystem by the reservoirs (the average number of reactions of a given type, multiplied by the associated chemical work, integrated over the whole process) in Supplementary Discussion 6. Throughout, we assume that receptor states are stable, and that reactions cannot occur without a catalyst. The eight steps of the cycle are intended to be closely analogous to the eight stages of the typical computational protocol in Supplementary Fig. 1; for subtleties involved in this comparison, see Supplementary Discussion 6. The system contains a readout (the memory bit) a receptor of known state R (a reference bit)

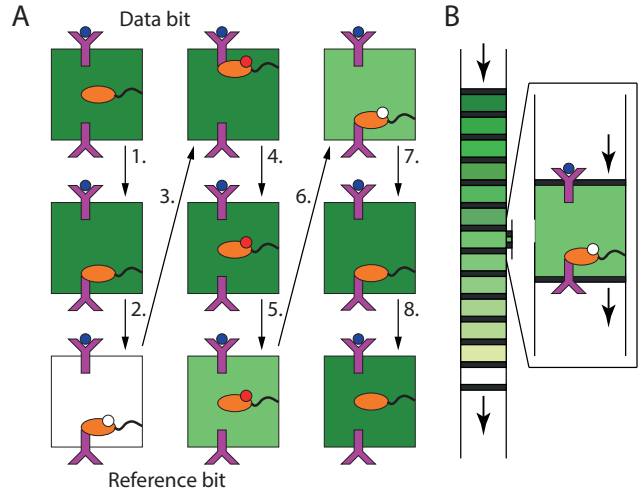


FIG. 5. A biochemical implementation of an optimal device and copy protocol. The cycle is illustrated in (A), and the steps are explained in the text. The system contains two receptors: one acting as a reference bit in state R for resetting and a receptor acting as a data bit in state RL or R . These receptors are attached to either end of a reaction volume. A readout molecule (memory bit) is tethered to the side of the reaction volume. The colour of the reaction volume indicates the chemical potential of fuel molecules in solution: it is dark when $\Delta G_p, \Delta G_d$ are large and negative and white when $\Delta G_p, \Delta G_d = 0$. (B) A device for implementing this cycle. A small reaction volume is coupled to a piston containing a series of reservoirs of varying ATP, ADP and P content. Similarly, the receptors and readout can be brought in and out of proximity by manipulation of a second piston.

and a receptor in either R or RL (the data bit).

The readout begins coupled to a buffer with $\Delta G_p, \Delta G_d = -\Delta G_r$ (ΔG_r assumed to be large and positive). There is no receptor in close proximity, but the readout has been reset (equilibrated at the end of a previous measurement cycle by a receptor in the R state), and therefore is in state x with probability $1/(1 + \exp(-\Delta G_r/kT))$. In fact, the accuracy of this reset does not influence the cost of the cycle (see Supplementary Discussion 6).

1. The readout is brought into close proximity with a receptor of known state R .
2. $\Delta G_p, \Delta G_d$ are slowly (quasistatically) raised from $-\Delta G_r$ to 0. Steps 1 and 2 allow the state of the memory to be reversibly uncorrelated from the reference receptor, prior to the measurement.
3. The readout is brought into close proximity with a receptor of unknown state (ligand-bound with probability p'). $\Delta G_p, \Delta G_d$ are then slowly lowered to $-\Delta G_s$. In this step, the state of the readout is set to match that of the receptor with accuracy $s = 1/(1 + \exp(-\Delta G_s/kT))$.
4. The readout is moved away from the receptor.

5. $\Delta G_p, \Delta G_d$ are set to ΔG_{off} . This stage constitutes the end of the copy subprocess; if the unknown receptor is in state RL , then the readout is in x^* with probability $s = 1/(1 + \exp(-\Delta G_s/kT))$. Similarly, if the unknown receptor is in state R , the readout is in x with probability $s = 1/(1 + \exp(-\Delta G_s/kT))$.
6. We now decorrelate the memory and data bits at a non-zero bias between the two readout states, $\Delta G_p, \Delta G_d = \Delta G_{\text{off}}$. To reach the fundamental thermodynamic bound, ΔG_{off} must be chosen carefully, and depends on p' and s . To decorrelate, the readout is brought into close proximity with a known receptor of state R . The readout relaxes to a state reflective of ΔG_{off} via the reaction $R + x^* \rightleftharpoons R + x + P$.
7. The readout molecule is reset by quasistatically lowering $\Delta G_p, \Delta G_d$ to $-\Delta G_r$ from ΔG_{off} , returning it to a state dominated by x .
8. The readout is separated from the reference bit, returning the system to the initial state.

The readout and receptor are in the same state at the start and finish of the cycle; thus the net chemical work of the reservoirs equates to the free energy dissipated by the entire system. As shown in Supplementary Discussion 6, minimizing dissipation with respect to ΔG_{off} at fixed p' and accuracy s (fixed by ΔG_s) gives a chemical work per copy equal to the mutual information generated by a measurement. In the special case $p' = 1/2$, $\Delta G_s \rightarrow \infty$, $w_{\text{chem}} \rightarrow kT \ln 2$, as expected. A single readout could also be made to copy multiple receptors sequentially – using, for example, a series of receptors anchored to a polymer, as in Supplementary Fig. 4. We note that it is also possible to construct an optimal cycle if the receptor is only catalytically active in the RL state – see Supplementary Fig. 5 and Supplementary Discussion 7.

II. DISCUSSION

We have described a canonical cellular readout network rigorously in terms of computational copy operations, thus demonstrating that the system is indeed bound by the thermodynamics of computation. For a general distribution of input data, the cellular network cannot reach this fundamental limit of efficiency. Unlike optimal computational protocols, the thermodynamic driving force used to push the memory device between its states is not introduced quasistatically. Instead, a continuously operating autonomous network must have a constant thermodynamic driving force. Even in the limit where the driving force and hence the accuracy become vanishingly small, the cellular system is not thermodynamically optimal. In the regime of high accuracy, the difference is larger: while optimal protocols can reach 100% accuracy for a finite cost of $kT \ln(2)$, cellular networks can only

achieve 100% accuracy for a cost that diverges. Nonetheless, achieving 99% accuracy for an unbiased distribution of input data requires less than $4kT \ln 2$ of dissipation per copy cycle, and the relative performance of the biochemical network for biased input data can be even better. Although kT sets an energy scale, it is not obvious *a priori* that the numerical factors should be so low. For example, the recently-derived “thermodynamic uncertainty relation”,⁴⁹ in which the cost of achieving a relative uncertainty ϵ in the number of steps of a biomolecular process was shown to be at least $2kT/\epsilon^2$ – gives $20000kT$ for 99% accuracy.

Not only can this canonical cellular signalling system get remarkably close to the fundamental bound for efficiency of copying at relatively high accuracy, it can do so at an arbitrarily high absolute copy rate. Further, the system is autonomous, and so there is no need to consider the intrinsic costs of applying a time-varying yet stable control to a bit, as must be done in typical protocols^{50,51}. Additionally, the canonical biochemical network naturally adapts to high or low levels of ligand-bound receptors, reducing its dissipation per copy cycle in a way that standard quasistatic protocols cannot achieve without feedback.

We have also explained the underlying reason why our mapping implies a minimal thermodynamic dissipation per copy for the network. This is not because the memory is “erased”, but because the correlations generated during measurement are not used to extract work. Erasure itself is not intrinsically irreversible, and no distinct erasure step is present.

Our analysis has revealed that biomolecules can in principle be used to implement protocols that achieve the thermodynamic bound, and we have provided an example. The key difference from the canonical cellular network is the manipulation of concentrations of ATP, ADP and P. If these manipulations are performed slowly enough, reactions (except decorrelation of readout and receptor) can be performed reversibly as reactants/products are gradually stabilised/destabilised with respect to each other.

In this work we have focussed on a single-step copy process. However, we have also argued that more complex copy processes, including multiple bound receptor/readout states or even multiple pathways in which different amounts of ATP can be consumed, cannot be equally accurate at a lower cost. Indeed, we have shown that all “tightly-coupled” processes in which all transitions consume the same amount of chemical fuel are equally efficient, and all others cannot perform better. At a physical level, it is intuitive that complex process can be less efficient – they naturally allow for dissipative cycles. Similarly, longer pathways are not helpful because one cannot make an irreversible process less irreversible by breaking it into many small steps whilst keeping the overall driving force fixed. For processes such as kinetic proofreading, however, in which chemical fuel drives reactions out of equilibrium, complex or longer reaction path-

ways can allow the same outcome at a lower cost.^{35,52,53} The crucial difference is that in a copy process, the metric of accuracy is exactly the ratio of forwards to backwards transition probabilities, which is the quantity directly influenced by fuel consumption. More fuel consumption always improves the metric. For other tasks, fuel consumption is necessary, but other factors can also influence performance. In kinetic proofreading, the relevant metric is the relative occupancy of a binding site by two different ligands.^{35,53} This quantity is influenced by the strength of chemical driving, but it is also limited by the number of intermediate states at which there is an opportunity to discriminate between ligands. Thus it can be beneficial to consider multi-stage proofreading.

Our analysis of the cellular network used the mean-field limit, which becomes accurate when the receptor correlation time τ_c is shorter than the relaxation time τ_r of the readout network. Interestingly, this is precisely the optimal regime for sensing²⁴, because the system can take multiple $\tau_r/\tau_c > 1$ concentration measurements per receptor molecule. In this regime, the readout molecules do not track the fluctuations in the receptor state, but, collectively, average it. As a result, the “learning rate”³⁸ between the readout and the receptor is actually zero in this limit (see Supplementary Discussion 1). While the opposite regime $\tau_r/\tau_c < 1$ is detrimental for the mechanism of time integration, we do note that the work per measurement is less. This is because in this regime the measurements become correlated, and taking correlated measurements requires less work for a given desired accuracy. A full analysis of this regime, as well as the consequences of spontaneous reactions not mediated by kinases and phosphatases, is the subject of further work.

The fact that cells employ thermodynamically inefficient out-of-equilibrium circuits highlights the constraints under which they function. Cells do not have infinite time to perform a measurement, meaning that quasistatic manipulations are infeasible. Further, our quasistatic protocol requires that a readout molecule exclusively encounters either ligand-bound *or* ligand-free receptors during each copy process. This requires that the ligand and ligand-free states of the receptors are stable on the time scale of the measurement cycle, and also that receptors in both states are not accessible to a single readout. In reality, the finite lifetime of receptor states places limits on the measurement time, and cells typically have multiple receptor molecules with which any one readout molecule can interact. The quasistatic cycle also necessitates coordinating the separation between readouts and receptors; although this is not inconceivable within a cell, it would require elaborate machinery. Perhaps most importantly, however, the quasistatic protocol requires manipulation of the concentration of chemical fuels; this manipulation must change chemical potentials by several kT to be effective. Given the relatively small number of chemical fuels available, and their extensive use in a range of systems, it would be very surprising if the cell manipulated chemical potentials purely for the

sake of measurement efficiency.

The final observation may also explain why cells use such a strong chemical driving (the hydrolysis of ATP typically provides approximately $20kT$, deep into the low error regime), rather than more efficiently taking measurements of only slightly lower accuracy²⁴. Indeed, the most efficient strategy from the perspective of sampling is to make many low-accuracy copies²⁴; this, however, requires time (for the measurements to be independent) and readout molecules (to store the measurements), resources which are not free for the cell.

Although motivated by the time integration of receptors by readouts, our analysis is also potentially applicable to other systems in which signals are propagated via chemical modification. Further, these ideas are also germane to synthetic biology and biological engineering in which the constraints and goals are distinct from those of natural systems. Additionally, we propose a new class of systems in which the fundamental thermodynamics of computation can be explored, to complement experiments done with optical or electrostatic feedback traps^{6,7} and magnetic systems⁸. Our approach involves manipulating biomolecules by adjusting the chemical potential of fuel molecules. Our experimental system is particularly promising because the dissipation could in principle be measured directly for a large number of devices acting in parallel rather than inferred from positional trajectories as it is done for the optical or feedback traps. In an experimental realization, it would be natural to treat the reservoirs and memory together as an extended system thermally coupled to the outside world. In this case the chemical free energy dissipated during measurement is not equal to the heat exchanged between the extended system and the outside world⁴⁵ – the increased entropy of the universe is instead manifest in a less uneven distribution of ATP, ADP and P between reservoirs. It would therefore be most natural to measure dissipation through the changing concentrations of ATP, ADP and P as the reservoirs exchange molecules – perhaps through radioactive labelling of phosphates. Further, it should be possible to perform full measurement cycles and probe the link between information loss and irreversibility. By measuring the state of the readout using, e.g., FRET, it would also be possible to test the generalized Jarzinsky equality, which shows that the state of the system can be changed more efficiently by exploiting knowledge of the state of the system^{54–56}.

III. METHODS

We analyse the biochemical network at the level of the chemical master equation. Reactants are assumed to be well-mixed and reactions occur with a propensity given by the concentration of reactants multiplied by a rate constant. Concentrations of ligand, ATP, ADP and P are assumed constant, and bound states of receptors and readouts short-lived. The master equation then reduces to instantaneous second order reactions between receptors and readouts, and first order interconversion of receptor states. We calculate the dissipation of the biochemical network at steady state and in

the mean-field limit, thereby assuming that receptor and readout states are uncorrelated. In the steady state, the dissipation rate is equal to the rate of chemical work done by the fuel (the net reactive flux multiplied by the drop in chemical potential of fuel molecules). The full master equation, the mean-field limit, and a discussion of the validity of this approximation are provided in Supplementary Discussion 1.

We compare the biochemical network to a two-state system in which computational operations are performed by external manipulation of the energy levels. An example is provided in Supplementary Fig. 1, and analysed in Supplementary Discussion 3. In this case, the work done during a protocol $\lambda(t)$ can be calculated^{46,57} as $\int d\lambda \partial \mathcal{H} / \partial \lambda$, in which \mathcal{H} is the internal energy of the system. This integral is simple to calculate for a two-state system in which manipulations are quasistatic, as demonstrated in Supplementary Discussion 3. In the case of the quasistatically-manipulated biochemical system, dissipation is calculated chemical work performed in one cycle (see Supplementary Discussion 6).

The dissipation is bounded by the mutual information I generated between the data and memory by copying. The mutual information between two stochastic variables X and Y is given by $I = \sum_{x,y} p(X=x, Y=y) \ln \left(\frac{p(X=x, Y=y)}{p(x=X)p(y=Y)} \right)$. This quantity is trivial to calculate for given input data and copy accuracy.

IV. REFERENCES

- ¹R. Landauer. Irreversibility and heat generation in the computing process. *IBM J. Res. Dev.*, 5:183–191, 1961.
- ²C. H. Bennett. Thermodynamics of computation - a review. *Int. J. Theor. Phys.*, 21:905–940, 1982.
- ³C. H. Bennett. Notes on Landauer's principle, reversible computation, and Maxwell's Demon. *Stud. Hist. Philos. M. P.*, 34:501–510, 2003.
- ⁴T. Sagawa and M. Ueda. Minimal energy cost for thermodynamic information processing: Measurement and information erasure. *Phys. Rev. Lett.*, 102:250602, 2009.
- ⁵B. Lambson, D. Carlton, and J. Bokor. Exploring the thermodynamic limits of computation in integrated systems: Magnetic memory, nanomagnetic logic, and the Landauer limit. *Phys. Rev. Lett.*, 107:010604, 2011.
- ⁶A. Bérut, A. Arakelyan, A. Petrosyan, S. Ciliberto, R. Dillenschneider, and E. Lutz. Experimental verification of Landauer's principle linking information and thermodynamics. *Nature*, 483(7388):187–189, 2012.
- ⁷Y. Jun, M. Gavrilov, and J. Bechhoefer. High-precision test of Landauer's principle in a feedback trap. *Phys. Rev. Lett.*, 113:190601, 2014.
- ⁸J. Hong, B. Lambson, S. Dhuey, and J. Bokor. Experimental verification of landauer's principle in erasure of nanomagnetic memory bits. *arXiv:1411.6730*, 2014.
- ⁹L. Szilard. On the decrease of entropy in a thermodynamic system by the intervention of intelligent beings. *Behav. Sci.*, 9:301–310, 1964.
- ¹⁰P. N. Fahn. Maxwell's demon and the entropy cost of information. *Found. Phys.*, 26:71–93, 1996.
- ¹¹M. B. Plenio and V. Vitelli. The physics of forgetting: Landauer's erasure principle and information theory. *Contemp. Phys.*, 42:25–60, 2001.
- ¹²J. Ladyman, S. Presnell, A. J. Short, and B. Groisman. The connection between logical and thermodynamic irreversibility. *Stud. Hist. Philos. M. P.*, 38:58 – 79, 2007.
- ¹³O.J.E. Maroney. The (absence of a) relationship between thermodynamic and logical reversibility. *Stud. Hist. Philos. M. P.*, 36:355 – 374, 2005.
- ¹⁴R. P. Feynman. *Feynman lectures on computation*. Addison-Wesley Publishing Co., Inc., New York, 1998.
- ¹⁵J. M. Parrondo, J. M. Horowitz, and T. Sagawa. Thermodynamics of information. *Nat. Phys.*, 11:131–139, 2015.
- ¹⁶H. C. Berg and E. M. Purcell. Physics of chemoreception. *Bioophys. J.*, 20:193, 1977.
- ¹⁷W. Bialek and S. Setayeshgar. Physical limits to biochemical signaling. *Proc. Nat. Acad. Sci. USA*, 102:10040, 2005.
- ¹⁸K. Wang, W.-J. Rappel, R. Kerr, and H. Levine. Quantifying noise levels in intercellular signals. *Phys. Rev. E*, 75:061905, 2007.
- ¹⁹W.-J. Rappel and H. Levine. Receptor noise and directional sensing in eukaryotic chemotaxis. *Phys. Rev. Lett.*, 100:228101, 2008.
- ²⁰R. G. Endres and N. S. Wingreen. Maximum likelihood and the single receptor. *Phys. Rev. Lett.*, 103:158101, 2009.
- ²¹B. Hu, W. Chen, W.-J. Rappel, and H. Levine. Physical limits on cellular sensing of spatial gradients. *Phys. Rev. Lett.*, 105:048104, 2010.
- ²²T. Mora and N. S. Wingreen. Limits of sensing temporal concentration changes by single cells. *Phys. Rev. Lett.*, 104:248101, 2010.
- ²³C. C. Govern and P. R. ten Wolde. Fundamental limits on sensing chemical concentrations with linear biochemical networks. *Phys. Rev. Lett.*, 109(21):218103, 2012.
- ²⁴C. C. Govern and P. R. ten Wolde. Optimal resource allocation in cellular sensing systems. *Proc. Nat. Acad. Sci. USA*, 111:17486–17491, 2014.
- ²⁵P. Mehta and D. J Schwab. Energetic costs of cellular computation. *Proc. Nat. Acad. Sci. USA*, 109:17978–17982, 2012.
- ²⁶C. C. Govern and P. R. ten Wolde. Energy dissipation and noise correlations in biochemical sensing. *Phys. Rev. Lett.*, 113:258102, 2014.
- ²⁷G. Lan, P. Sartori, S. Neumann, V. Sourjik, and Y. Tu. The energy-speed-accuracy trade-off in sensory adaptation. *Nat. Phys.*, 8:422–428, 2012.
- ²⁸S. Sartori, L. Granger, C. Fan Lee, and J. M. Horowitz. Thermodynamic costs of information processing in sensory adaption. *PLoS Comput. Biol.*, 10:e1003974, 2014.
- ²⁹S. Ito and T. Sagawa. Maxwell's demon in biochemical signal transduction with feedback loop. *Nat. Comm.*, 6:7498, 2015.
- ³⁰J. J. Hopfield. Kinetic proofreading: a new mechanism for reducing errors in biosynthetic processes requiring high specificity. *Proc. Nat. Acad. Sci. USA*, 71:4135–4139, 1974.
- ³¹G. De Palo and R. G Endres. Unraveling adaptation in eukaryotic pathways: Lessons from protocells. *PLoS Comp. Biol.*, 9:e1003300, 2013.
- ³²A. C. Barato, D. Hartich, and U. Seifert. Information-theoretic versus thermodynamic entropy production in autonomous sensory networks. *Phys. Rev. E*, 87:042104, 2013.
- ³³M. Skoge, S. Naqvi, Y. Meir, and N. S. Wingreen. Chemical sensing by nonequilibrium cooperative receptors. *Phys. Rev. Lett.*, 110:248102, 2013.
- ³⁴J. Ninio. Kinetic amplification of enzyme discrimination. *Biochimie*, 57(5):587–595, 1975.
- ³⁵H. Qian. Reducing intrinsic biochemical noise in cells and its thermodynamic limit. *J. Mol. Biol.*, 362:387–392, 2006.
- ³⁶A. M Stock, V. L Robinson, and P. N. Goudreau. Two-component signal transduction. *Ann. Rev. Biochem.*, 69:183–215, 2000.
- ³⁷K. Kaizu, W. de Ronde, J. Pajjmans, K. Takahashi, F. Tostevin, and P. R. ten Wolde. The berg-purcell limit revisited. *Biophysical journal*, 106(4):976–985, 2014.
- ³⁸A. C. Barato, D. Hartich, and U. Seifert. Efficiency of cellular information processing. *New J. Phys.*, 16:103024, 2014.
- ³⁹D. Hartich, A. C. Barato, and U. Seifert. Stochastic thermodynamics of bipartite systems: transfer entropy inequalities and a maxwell's demon interpretation. *J. Stat. Mech. Theor. and Exp.*, 2014:P02016, 2014.
- ⁴⁰J. M. Horowitz and M. Esposito. Thermodynamics with continuous information flow. *Phys. Rev. X*, 4:031015, 2014.
- ⁴¹J. M. Horowitz, T.o Sagawa, and J. M. R. Parrondo. Imitating

chemical motors with optimal information motors. *Phys. Rev. Lett.*, 111:010602, 2013.

⁴²L. Granger and H. Kantz. Differential Landauer's principle. *Europhys. Lett.*, 101:50004, 2013.

⁴³R. J. Allen, C. Valeriani, and P. R. ten Wolde. Forward flux sampling for rare event simulations. *J. Phys.: Condens. Matter*, 21:463102, 2009.

⁴⁴G. E. Crooks. Entropy production fluctuation theorem and the nonequilibrium work relation for free energy differences. *Phys. Rev. E*, 60:2721, 1999.

⁴⁵U. Seifert. Stochastic thermodynamics of single enzymes and molecular motors. *Eur. Phys. J. E*, 34:26, 2011.

⁴⁶U. Seifert. Stochastic thermodynamics, fluctuation theorems and molecular machines. *Rep. Prog. Phys.*, 75:126001, 2012.

⁴⁷R. Kawai, J. M. R. Parrondo, and C. Van den Broeck. Dissipation: The phase-space perspective. *Phys. Rev. Lett.*, 98:080602, 2007.

⁴⁸A. Gomez-Marin, J. M. R. Parrondo, and C. Van den Broeck. Lower bounds on dissipation upon coarse graining. *Phys. Rev. E*, 78:011107, 2008.

⁴⁹A. C. Barato and U. Seifert. Thermodynamic uncertainty relation for biomolecular processes. *Phys. Rev. Lett.*, 114:158101, 2015.

⁵⁰M. Gopalkrishnan. Personal Communication.

⁵¹B. B. Machta. Dissipation bound for thermodynamic control. *Phys. Rev. Lett.*, 115:260603, 2015.

⁵²A. H. Lang, C. K. Fisher, and P. Mehta. Thermodynamics of statistical inference by cells. *Phys. Rev. Lett.*, 113:148103, 2014.

⁵³M. Ehrenberg and C. Blomberg. Thermodynamic constraints on kinetic proofreading in biosynthetic pathways. *Biophys. J.*, 31:333–358, 1980.

⁵⁴S. Toyabe, T. Sagawa, M. Ueda, E. Muneyuki, and M. Sano. Experimental demonstration of information-to-energy conversion and validation of the generalized Jarzynski equality. *Nat. Phys.*, 6:988–992, 2010.

⁵⁵V. Koski, J. F. Maisi, V. T. Sagawa, and P. Pekola, J. Experimental observation of the role of mutual information in the nonequilibrium dynamics of a maxwell demon. *Phys. Rev. Lett.*, 113:030601, 2014.

⁵⁶É. Roldán, I. A. Martínez, J. M. R. Parrondo, and D. Petrov. Universal features in the energetics of symmetry breaking. *Nat. Phys.*, 10:457–461, 2014.

⁵⁷K. Sekimoto. Langevin equation and thermodynamics. *Prog. Theor. Phys. Supp.*, 130:17–27, 1998.

Acknowledgements: We thank Giulia Malaguti for a critical reading of the manuscript and Andrew Turberfield for helpful discussions. This work is part of the research programme of the Foundation for Fundamental Research on Matter (FOM), which is part of the Netherlands Organisation for Scientific Research (NWO).

Appendix A: The master equation of the biochemical network

The model presented in Eq. 2 of the main text defines a master equation for the variables x^* and RL , the number of phosphorylated readouts and ligand-bound receptors, respectively.

$$\begin{aligned} \frac{dP(x^*, RL)}{dt} = & -([L]k_1(R_T - RL) + k_2RL)P(x^*, RL) \\ & + [L]k_1(R_T - (RL - 1))P(x^*, RL - 1) + k_2(RL + 1)P(x^*, RL + 1) \\ & - \left((k_3 \frac{RL}{V} + k_5 \frac{R_T - RL}{V})(x_T - x^*) + (k_4 \frac{RL}{V} + k_6 \frac{R_T - RL}{V})x^* \right) P(x^*, RL) \\ & + (k_3 \frac{RL}{V} + k_5 \frac{R_T - RL}{V})(x_T - (x^* - 1))P(x^* - 1, RL) + (k_4 \frac{RL}{V} + k_6 \frac{R_T - RL}{V})(x^* + 1)P(x^* + 1, RL), \end{aligned} \quad (\text{A1})$$

in which V is the system volume. We assume that the ligand concentration is large enough that $[L]$ is uninfluenced by RL – thus $\tilde{k}_1 = k_1[L]$ is a constant. We also assume that bound states formed between receptors and downstream proteins are short-lived compared to the typical time between binding events, so that all receptor/readout reactions are essentially instantaneous. This is equivalent to assuming that the probability of finding the memory in between the wells (at the top of the barrier) is negligible in the computational device in Supplementary Figure 1. In this work, we are interested in the steady state. Firstly, it is trivial to see that RL does not depend on x^* . Due to the linearisation that arises from assuming $k_1[L] = \tilde{k}_1$, the stationary distribution for $P(RL)$ is a simple binomial:

$$P(RL) = \left(\frac{\tilde{k}_1}{\tilde{k}_1 + k_2} \right)^{RL} \left(\frac{k_2}{\tilde{k}_1 + k_2} \right)^{R_T - RL} \frac{R_T!}{(R_T - RL)!RL!}, \quad (\text{A2})$$

with mean $\langle RL \rangle / R_T = p = \tilde{k}_1 / (\tilde{k}_1 + k_2)$. Finding the full solution, $P(x^*, RL) = P(x^*|RL)P(RL)$, is more challenging due to non-linearities that remain in the reactions involving phosphorylation and dephosphorylation of x . However, we do note that the behaviour of each readout molecule is independent of the other readouts, and thus

$$P(x^*|RL) = q(*|RL)^{x^*} (1 - q(*|RL))^{x_T - x^*} \frac{x_T!}{x^*!(x_T - x^*)!}, \quad (\text{A3})$$

in which $q(*|RL)$ is the probability that a single readout is phosphorylated in a system with R_T receptors, given that RL of them are ligand-bound. Note that this holds when RL fluctuates in time. Even the calculation of $q(*|RL)$ is non-trivial, however, and we do not attempt it here.

1. Mean-field approximation

To derive Eqs. 11 and 12 of the main text, we make the mean-field assumption that fluctuations in x^* are uncorrelated with fluctuations in RL . Mathematically, we assume $P(x^*|RL) = P(x^*|\langle RL \rangle) = P(x^*)$. We combine this assumption with the fact that, as x^* is a 1d variable with reflecting boundary conditions, the total flux associated the increment $x^* \rightarrow x^* + 1$ must cancel with the total flux associated with $x^* + 1 \rightarrow x^*$. At the mean-field level of approximation, this condition yields

$$\left(k_4 \frac{\langle RL \rangle}{V} + k_6 \frac{R_T - \langle RL \rangle}{V} \right) (x^* + 1) P(x^* + 1) = \left(k_3 \frac{\langle RL \rangle}{V} + k_5 \frac{R_T - \langle RL \rangle}{V} \right) (x_T - x^*) P(x^*). \quad (\text{A4})$$

By summing over x^* , we obtain the following expression for $\langle x^* \rangle$:

$$\left(k_4 \frac{\langle RL \rangle}{V} + k_6 \frac{R_T - \langle RL \rangle}{V} \right) \langle x^* \rangle = \left(k_3 \frac{\langle RL \rangle}{V} + k_5 \frac{R_T - \langle RL \rangle}{V} \right) (x_T - \langle x^* \rangle), \quad (\text{A5})$$

and therefore

$$f = \frac{\langle [x^*] \rangle}{[x_T]} = \frac{k_3 p + k_5 (1-p)}{(k_3 + k_4)p + (k_5 + k_6)(1-p)}, \quad (\text{A6})$$

as quoted in Eq. 12 of the main text. Further, the average flux of readouts around the cycle is given by

$$\dot{n}_{\text{flux}} = \frac{k_3}{V} \langle RLx \rangle - \frac{k_4}{V} \langle RLx^* \rangle = k_3 p R_T [x_T] - \frac{k_3 + k_4}{V} \langle RLx^* \rangle. \quad (\text{A7})$$

In our approximation, $\langle RLx^* \rangle = \langle RL \rangle \langle x^* | RL \rangle$ and thus

$$\dot{n}_{\text{flux}} = (k_3(1-f) - k_4 f) p [x_T] R_T, \quad (\text{A8})$$

as stated in Eq. 11 of the main text. For completeness, we also give the differential equations that govern RL and x^* in the limit of deterministic chemical kinetics:

$$\begin{aligned} \frac{dRL}{dt} &= -k_2 RL + \tilde{k}_1 (R_T - RL), \\ \frac{dx^*}{dt} &= -(k_4[RL] + k_6([R_T] - [RL]))x^* + (k_3[RL] + k_5([R_T] - [RL]))(x_T - x^*). \end{aligned} \quad (\text{A9})$$

The steady state of these deterministic equations is given by the stationary stochastic averages in the mean-field approximation: $RL = \langle RL \rangle$ and $x^* = \langle x^* | RL \rangle$.

The mean-field limit is valid when the number of receptors is large, so that fluctuations about the average are negligible (note that the number of readouts does not have to be large). The mean-field limit is also valid when the kinetics of receptors is fast compared to that of the readouts – in this case, $P(x^*|RL) = P(x^*|\langle RL \rangle) = P(x^*)$ since the receptors fluctuate too rapidly to be tracked by the readouts. Indeed, the master equation can be readily solved for a single receptor and a single readout, with the steady-state solution

$$\begin{aligned} P(x^* = 0, RL = 0) &= \frac{k_2(\tilde{k}_1 k_4' + k_2 k_6' + k_3 k_6' + k_4' k_6')}{C}, \\ P(x^* = 1, RL = 0) &= \frac{k_2(\tilde{k}_1 k_3' + k_2 k_5' + k_3 k_5' + k_4' k_5')}{C}, \\ P(x^* = 0, RL = 1) &= \frac{k_1[L](\tilde{k}_1 k_4' + k_2 k_6' + k_4' k_6' + k_4' k_5')}{C}, \\ P(x^* = 1, RL = 1) &= \frac{\tilde{k}_1(\tilde{k}_1 k_3' + k_2 k_5' + k_3 k_5' + k_3 k_6')}{C}, \end{aligned} \quad (\text{A10})$$

in which $k_i' = k_i/V$, and C is a normalizing constant. In the limit $\tilde{k}_1, k_2 \gg k_3', k_4', k_5', k_6'$, the net flux can be directly evaluated as

$$k_3' P(x^* = 0, RL = 1) - k_4 P(x^* = 1, RL = 1) = \frac{(k_3' k_6' - k_4' k_5')p(1-p)}{p(k_3' + k_4') + (1-p)(k_5' + k_6')} = \frac{(k_3 k_6 - k_4 k_5)p(1-p)[x_T] R_T}{p(k_3 + k_4) + (1-p)(k_5 + k_6)}, \quad (\text{A11})$$

consistent with Eqs. 11 and 12 of the main text.

Finally, the mean field limit also holds if the receptors do not fluctuate at all – *i.e.*, if RL is fixed over time at a given value. Such a system (which would be a poor concentration sensor) would be equivalent to a system with a fixed number of constitutively active kinases and a fixed number of constitutively active phosphatases. In this case, the fixed value of RL/R_T determines p , rather than the average of the ligand binding and unbinding dynamics. However, the equations for x^* and \dot{n}_{flux} hold exactly given this value of p . Note that this situation is not equivalent to slow but finite receptor dynamics, in which RL still fluctuates for a given system.

2. Mapping to the copy process does not require the mean-field approximation

The mapping between an abstract system that performs copies and the biochemical network in Eqs. 3-5 of the main text was performed at the level of transition rates in the Markov model. It is therefore not dependent on a mean-field approximation. We also note that the expression for the average rate at which copies are made,

$$\dot{n}_{\text{copy}} = \langle k_{\text{copy}}^{RL} x_T + k_{\text{copy}}^R x_T \rangle = \langle \frac{k_3 + k_4}{V} RL x_T + \frac{k_5 + k_6}{V} Rx_T \rangle = ((k_3 + k_4)p + (k_5 + k_6)(1 - p))R_T[x_T], \quad (\text{A12})$$

does not rely on a mean-field approximation.

3. Violation of mean field behavior

For low numbers of receptors and slow receptor dynamics, the approximation $P(x^*|RL) = P(x^*|\langle RL \rangle) = P(x^*)$ breaks down. In this case, $\langle RLx^* \rangle > \langle RL \rangle \langle x^* | RL \rangle$, since a greater number of ligand-bound receptors leads to more phosphorylation. The result is that \dot{n}_{flux} is lower than under the mean-field assumption. Since the expression for the rate of copying remains valid,

$$\frac{w_{\text{chem}}}{n_{\text{copy}}} < \frac{(k_3 k_6 - k_4 k_5)p(1 - p)}{((k_3 + k_4)p + (k_5 + k_6)(1 - p))^2} kT \ln \left(\frac{k_3 k_6}{k_4 k_5} \right). \quad (\text{A13})$$

Physically, the cost of a copy cycle is reduced because the state of the readout is correlated with the receptor prior to copying. This means that fewer actual phosphorylation/dephosphorylation events occur per copy cycle, and hence less dissipation is necessary. Our comparison to copying, and the calculation of the information generated, assume the measurement of uncorrelated data bits; a lower cost for copying of correlated data bits can also be achieved with the ideal device in Supplementary Fig. 1. To do this, the decorrelation step 6 in Supplementary Fig. 1 must not be allowed to run to completion – the barrier between wells should be raised after a certain finite time. The memory bit should then be exposed directly to the next data bit (step 3 in the quasistatic protocol), and the barrier between wells only lowered when the strength of interaction between memory and data bits reflects the correlation between successive data bits. For example, if the correlation between subsequent data bits tends towards unity, the optimal protocol would retain the memory bit in the state of the previous data bit by reducing the time spent in step 6 towards zero. The memory bit would then be exposed to the data bit, but the barrier between wells is not lowered until the coupling is extremely strong. In the limit of perfect correlation, this procedure would require no work. A full exploration of the correlated regime is beyond the scope of this paper, due to its additional complexity. We note in passing that correlated copies of the receptors are not helpful in sensing²⁴, and indeed the readout molecules need to respond slowly in order to perform time integration²⁴. The regime in which the readout transitions are slower than those of the receptor state not only makes the mean-field analysis accurate, but is also the biologically relevant regime.

4. Learning rate in the mean-field limit

The “learning rate”³⁸ gives the rate at which transitions in one part of a bi-partite reaction network act to increase the mutual information between that part of the network and the other part. The most obvious application to a sensory system such as discussed in our manuscript would be to calculate the learning rate that results from the biochemical network’s response to changes in the concentration $[L]$. This would be highly relevant to the quality of the network as a sensor of dynamic concentrations. However, it is not of direct relevance here, as we are concerned with whether the action of the readouts can truly be related to computational copying, and if so, how the efficiency relates to thermodynamic bounds on copying. This learning rate would depend both on the steady-state distribution and dynamics of $[L]$. The receptors and readouts also form a bi-partite system, and hence a learning rate can be

defined here. The parameters of the model specify a learning rate, but to calculate it would require the evaluation of $P(x^*, RL)$. In the mean-field limit we can show that the learning rate is zero. The learning rate is³⁸

$$l = - \sum_{x^*, RL} P(x^*, RL) \sum_{x^{*\prime} \neq x^*} w_{x^*, x^{*\prime}}^{RL} \ln \left(\frac{P(x^*, RL)}{P(x^{*\prime}, RL)} \right), \quad (\text{A14})$$

which, using our mean-field approximation, can be re-written as

$$l = - \sum_{x^*} \sum_{x^{*\prime} \neq x^*} P(x^*) W_{x^*, x^{*\prime}} \ln \left(\frac{P(x^*)}{P(x^{*\prime})} \right), \quad (\text{A15})$$

in which $W_{x^*, x^{*\prime}} = \sum_{RL} P(RL) w_{x^*, x^{*\prime}}^{RL}$. The variable $w_{x^*, x^{*\prime}}$ is only non-zero for adjacent values of x^* and $x^{*\prime}$. Further, in the steady state, the average flow from x^* to $x^{*\prime}$ must cancel. Therefore we obtain a balance condition that holds for all $x^*, x^{*\prime}$:

$$\sum_{RL} P(x^*, RL) w_{x^*, x^{*\prime}}^{RL} - P(x^{*\prime}, RL) w_{x^{*\prime}, x^*}^{RL} = 0. \quad (\text{A16})$$

Applying the mean-field approximation to the above expression gives

$$P(x^*) W_{x^*, x^{*\prime}} = P(x^{*\prime}) W_{x^{*\prime}, x^*}. \quad (\text{A17})$$

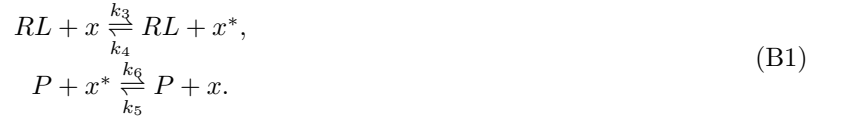
Substituting Eq. A17 into Eq. A15 gives

$$l = \sum_{x^*, x^{*\prime}, x^{*\prime} \neq x^*} P(x^*) W_{x^*, x^{*\prime}} \ln (P(x^*)) - P(x^{*\prime}) W_{x^{*\prime}, x^*} (P(x^{*\prime})) = 0. \quad (\text{A18})$$

The fact that the learning rate between receptors and readouts is zero in the mean field limit is consistent with the argument in the previous subsection. In the mean field limit, receptors are perfectly time-averaging, instead of responding to fluctuations; the learning rate reports the degree to which x^* responds to fluctuations in RL .

Appendix B: Receptors that only act as kinases in the canonical biochemical network

In the main text we considered a canonical biochemical system in which receptors were bifunctional – RL acted as kinases, and R as phosphatases. An alternative is a system in which RL act as kinases but R are inactive, and constitutively active phosphatases exist within the cell. At the level of second-order rate constants, our reactions are:



In this system, it is not the state of the receptor that is copied into the readout, as R is completely passive. Instead, enzyme identities RL or P are copied into the state of the readout as x^* or x respectively, in the same way that RL and R were copied in the bifunctional system. The relative frequency with which each copy happens can be used to estimate ligand concentration. Eqs. 11 and 12 of the main text still hold, but the average fraction f of phosphorylated readout in the mean-field limit is

$$f = \frac{k_3 p R_T + k_5 P_T}{(k_3 + k_4) p R_T + (k_5 + k_6) P_T}, \quad (\text{B2})$$

in which P_T is the total number of phosphatases. Thus

$$\dot{w}_{\text{chem}} = \frac{(k_3 k_6 - k_4 k_5) p [x_T] P_T R_T}{(k_3 + k_4) p R_T + (k_5 + k_6) P_T} k T \ln \left(\frac{k_3 k_6}{k_4 k_5} \right). \quad (\text{B3})$$

Analogously to the system considered in the main text, the rate at which copies are attempted is

$$\dot{n}_{\text{copy2}} = [x_T] ((k_3 + k_4) p R_T + (k_5 + k_6) P_T). \quad (\text{B4})$$

Combining Equations B3 and B4, the dissipation of free energy per copy cycle in the mean-field limit is given by

$$\frac{w_{\text{chem}}}{n_{\text{copy}}} = \frac{(k_3 k_6 - k_4 k_5) p P_T R_T}{((k_3 + k_4) p R_T + (k_5 + k_6) P_T)^2} kT \ln \left(\frac{k_3 k_6}{k_4 k_5} \right). \quad (\text{B5})$$

Further,

$$p' = p \frac{(k_3 + k_4) R_T}{(k_3 + k_4) p R_T + (k_5 + k_6) P_T} \quad (\text{B6})$$

is the probability that an attempted copy is of *RL* rather than *P*, and

$$s_{RL} = \frac{k_3}{k_3 + k_4}, \quad s_P = \frac{k_6}{k_5 + k_6} \quad (\text{B7})$$

are the accuracies with which *RL* and *P* are copied, respectively.

The results are closely analogous to those obtained in the main text for the canonical biochemical network, and in fact are related by the transformation $(1 - p)R_T \rightarrow P_T$ (which is perhaps unsurprising). Indeed, $w_{\text{chem}}/n_{\text{copy}}$ is the same function of p' in both cases

$$\frac{w_{\text{chem}}}{n_{\text{copy}}} = (s_1 + s_2 - 1)p'(1 - p')(E_{s_{RL}} + E_{s_P}). \quad (\text{B8})$$

Thus our analysis in the main text still holds, except for the fact that the phosphatase concentration is not directly controlled by varying the probability of receptor-ligand binding p . A given cell operating without bi-functional receptors, therefore, does not automatically adapt to high p by converting all phosphatases to kinases, and so will not use a vanishing free-energy per copy cycle at high p (because p' does not tend towards 1, unlike in the bi-functional system). Its behaviour as a function of p' , however, is identical.

Appendix C: A typical computational device and protocol

Here we outline a non-autonomous computational protocol for copying/measurement that reaches the thermodynamic bound of efficiency for a process that performs copies with a given accuracy $s = s_R = s_{RL} = 1/(1 + \exp(-E_s/kT))$, and subsequently allows the information to be lost in an uncontrolled fashion. We shall initially consider a process that reaches the bound when copying data which is in state 1 with a probability $p' = 0.5$, before subsequently generalising.

The prototypical memory device is a system capable of storing binary information reliably for a long time: a *memory bit*. The state of the memory bit can be altered by coupling it to external systems; it is important that the memory bit persists in the altered state after the coupling is removed. We shall also manipulate the memory bit using a system of known state, a *reference bit*, that allows the memory bit to be reset to a standard state.

The computational device and protocol discussed here is based on that of Bennett². Our memory bit is a single particle in a double-well energy landscape, as illustrated in Supplementary Fig.1^{2,3,14}. A particle in the left well is in state 0, a particle in the right well is in state 1. Coupling the memory bit to an external bit in state 0 raises the right-hand well (stronger coupling implies a larger shift), whereas coupling the memory to an external bit in state 1 raises the left-hand well. The barrier between the wells of the memory bit can be lowered and raised as desired.

1. Special case for $p' = 0.5$

The protocol is illustrated in Supplementary Fig. 1. The memory bit starts in state 0 (the left well) with a probability $1/(1 + \exp(-E_r/kT))$, due to having been equilibrated by a reference bit in state 0 at a coupling strength E_r (the accuracy of this initial reset will turn out to be irrelevant for the cost). The data bit is then copied into the memory bit (steps 1-5). Steps 6-8 return the memory to the standard state 0 prior to the next measurement. In step 6, the memory and data bits decorrelate, before the actual reset in step 7 and the raising of the barrier in step 8.

To calculate the work done in the protocol, we make the following assumptions. We will assume that the barrier is large enough that hopping between the wells is negligible on all relevant timescales unless the barrier is deliberately lowered. We will also assume that the wells are broad and steep-sided so that the potential energy of a particle in either well is well-defined. Finally, we assume that raising/lowering the barrier does no work because the probability of finding the particle at the top of the barrier is always negligible (we are considering an ideal two-state system).

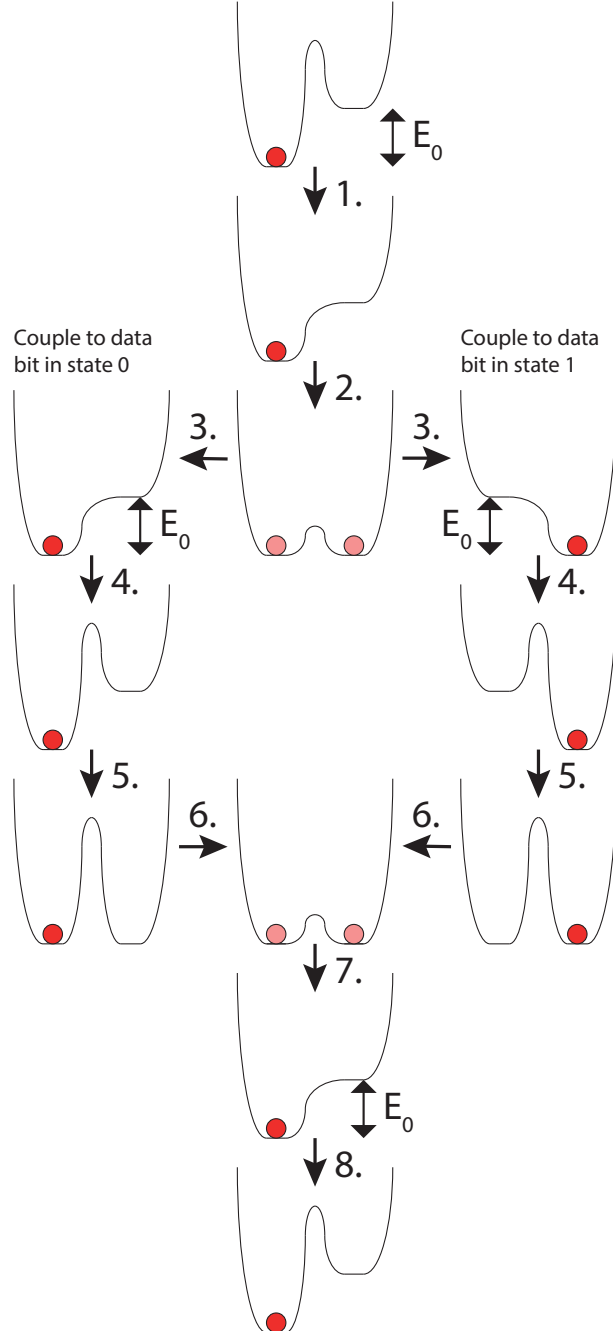


FIG. 6. **Supplementary Figure 1:** A canonical computational measurement/copy cycle with a particle in a double well potential representing a memory bit. The particle starts in state 0 (the left well) with the energy of the right well raised by $E_0 \gg kT$ due to coupling of the memory to a reference bit. Step 1: the barrier between wells is lowered. Step 2: The memory is slowly decoupled from the reference bit, allowing the right well to fall. The particle remains in equilibrium between the two wells. Step 3: the memory is gradually coupled to a data bit of unknown state, raising either the left or the right well. Step 4: the barrier between the wells is raised. Step 5: the memory and data bits are decoupled, completing the copy stage of the protocol. Steps 6-8 are performed prior to the next copy to return the memory bit to state 0. Step 6: the barrier between wells is lowered, allowing the particle to equilibrate between the wells. Step 7: the memory is gradually coupled to the reference bit, and the particle is returned to the left well. Step 8: the barrier is raised, returning the memory bit to its initial state 0. Steps 1-5 constitute the copy protocol, step 6 is decorrelation, and steps 7 and 8 are the resetting of the memory.

For conceptual convenience, we begin our description in state 0, coupled to the reference bit that has been used to reset the memory bit after the last measurement. This choice aligns the start of our cycle with the start of the copy sub-process (the first five stages of the cycle). A reasonable alternative would be to start our description at step 6, so that our measurement procedure begins with setting the memory bit to 0 (steps 6-8) and subsequently involves a copy (steps 1-5). This arbitrary choice is of no fundamental importance. Proceeding step-by-step:

1. The barrier is lowered; no work is done.
2. The right well is slowly (quasistatically) lowered from E_r to 0 as the coupling of the memory bit to a reference bit of known state 0 is reduced. Here, slowness is measured relative to the relaxation time of the system; it is assumed that at any instant, the memory is in a state that is representative of equilibrium given the instantaneous energy landscape. The average work done in this protocol is^{46,57}

$$w_2 = \int_{E_r}^0 \frac{e^{-E'/kT}}{1 + e^{-E'/kT}} dE' = -kT \ln \left(\frac{2}{1 + e^{-E_r/kT}} \right), \quad (C1)$$

which tends to $-kT \ln 2$ in the limit $E_r/kT \rightarrow \infty$. This result shows why the presence of the reference bit at the start of the copy is necessary. Had we instead performed steps 1 and 2 in reverse, lowering the right well to 0 and then lowering the barrier (equivalent to initiating the measurement without a reference bit present), we would have allowed the memory bit to relax freely to the 50/50 state. The work extracted would have been zero, increasing the total work done during a cycle (by $kT \ln 2$ as $E_r/kT \rightarrow \infty$).

3. The memory is exposed to the data bit; as the coupling of the memory bit to the data bit increases, either the left or right well rises from 0 to E_s depending on the state of the data bit. The average work done by slowly coupling the memory to the data bit is

$$w_3 = \int_0^{E_s} \frac{e^{-E'/kT}}{1 + e^{-E'/kT}} dE' = kT \ln \left(\frac{2}{1 + e^{-E_s/kT}} \right), \quad (C2)$$

which tends to $kT \ln 2$ in the limit $E_s/kT \rightarrow \infty$.

4. The barrier is raised; no work is done
5. The system is decoupled from the data bit, lowering the well that was previously raised. If E_s is finite, there is a finite probability of the particle being in this “wrong” well; the work done on the system is

$$w_5 = -\frac{e^{-E_s/kT}}{1 + e^{-E_s/kT}} E_s, \quad (C3)$$

which tends to 0 in the limit $E_s/kT \rightarrow \infty$. This subprocess completes the copying stage of the measurement protocol; the remaining stages involve setting the memory bit to 0 ahead of the next measurement. The probability of performing a correct copy is $1/(1 + \exp(-E_s/kT)) = s$, as required.

6. The barrier is lowered. The memory bit becomes decorrelated from the data bit. The total entropy of memory and data bits therefore increases, but no work is done. In the limit $E_0 \rightarrow \infty$, the memory and data bits are perfectly correlated prior to this step. Therefore the possible configurations of the memory and data bits change from (0,0) or (1,1) to (0,0), (0,1), (1,0) or (1,1), an entropy increase of $k \ln 2$.
7. The memory is reset by slowly coupling to a reference bit of state 0. The average work done is

$$w_7 = \int_0^{E_r} \frac{e^{-E'/kT}}{1 + e^{-E'/kT}} dE' = kT \ln \left(\frac{2}{1 + e^{-E_r/kT}} \right), \quad (C4)$$

which tends to $kT \ln 2$ in the limit $E_r/kT \rightarrow \infty$.

8. The barrier is raised; no work is done. The memory bit has been reset to state 0 with probability $1/(1 + \exp(-E_r/kT))$.

The total work done during this cycle is

$$w_T = kT \ln \left(\frac{2}{1 + e^{-E_s/kT}} \right) - \frac{e^{-E_s/kT}}{1 + e^{-E_s/kT}} E_s. \quad (C5)$$

As the state of the system is unchanged at the end of the cycle, this work is dissipated irreversibly. If $p' = 1/2$, and the accuracy of copying is $s_R = s_{RL} = s$, the information generated by the copy process is

$$I = s \ln(2s) + (1-s) \ln(2(1-s)) = \ln(2s) + (1-s) \ln\left(\frac{1-s}{s}\right) = w_T/kT. \quad (\text{C6})$$

The final equality follows from the definition of E_s in terms of s , $E_s = kT \ln(s/(1-s))$ or equivalently $s = 1/(1 + \exp(-E_s/kT))$. Thus the protocol reaches the thermodynamic bound on dissipation for copying data with $p' = 1/2$ at an accuracy of s .

In the main text, we contrasted the cost of the biochemical network and the optimal protocol for $p' = 0.5$, $s_r = s_{RL} = s$ by considering the (free-) energy drops associated with the transitions of the memory. In fact, this is the heat associated with the transitions (or the total drop in chemical free energy of the entire system). One can derive the same cost per copy (Eq. C5) for an optimal protocol by considering this heat transfer instead of work. For $p' = 0.5$, $s_r = s_{RL} = s$, the net heat transfer is given entirely by the heat transferred in step 4; steps 2 and 7 cancel, and the heat is zero for other steps. This is why the intuitive discussion in the main text, which only considers the actual transitions of the memory by which it is set to match the data, is valid.

2. Generalising to $p' \neq 0.5$

It is clear from the fact that Eq. C5 does not depend on the distribution of input data that the above protocol is not optimal for all p' . In this protocol, we made the implicit decision to perform decorrelation (step 6) in a state in which there is no bias between the two wells. We could, instead, consider performing decorrelation by first coupling the memory to another reference bit in state 1 with coupling strength E_{off} , then lowering the barrier to allow decorrelation, and finally quasistatically reducing the offset to 0 prior to proceeding with the reset.

There is no change to stages 1-5 or 7-8, in which the total work performed is

$$w_{1-5} + w_{7-8} = kT \ln\left(\frac{2}{1 + \exp(-E_s/kT)}\right). \quad (\text{C7})$$

It is now necessary to raise left well (state 0) by an energy E_{off} , perform the decorrelation, lower the left well back to 0 and finally raise the right well to E_s . The work done in raising the left well is

$$w_{6a} = (1-f)E_{\text{off}}, \quad (\text{C8})$$

since a particle will be in the left well after the measurement with a probability $1-f$ by definition ($f = p's + (1-p')(1-s)$ is the probability of a measurement outcome being 1). No work is done during the decorrelation stage, and in lowering the left well quasistatically to 0 the work done is

$$w_{6c} = \int_{E_{\text{off}}}^0 dE \frac{\exp(-E/kT)}{1 + \exp(-E/kT)} = -kT \ln\left(\frac{2}{1 + \exp(-E_{\text{off}}/kT)}\right). \quad (\text{C9})$$

Summing over all contributions gives a total work during the cycle of

$$w_T = kT \ln\left(\frac{1 + e^{-E_{\text{off}}/kT}}{1 + e^{-E_s/kT}}\right) - \frac{e^{-E_s/kT}}{1 + e^{-E_s/kT}} E_s + (1-f)E_{\text{off}}. \quad (\text{C10})$$

At fixed p' and s (and hence f), this expression is minimised by

$$1 - f - \frac{e^{-E_{\text{off}}^{\dagger}/kT}}{1 + e^{-E_{\text{off}}/kT}} = 0. \quad (\text{C11})$$

Hence the optimal decorrelation energy is

$$E_{\text{off}}^{\dagger} = kT \ln(f/(1-f)), \quad (\text{C12})$$

for which the work is

$$w_T^{\dagger} = kT (s \ln s + (1-s) \ln(1-s)) - kT (f \ln f + (1-f) \ln(1-f)). \quad (\text{C13})$$

In other words, decorrelation should be performed at a bias that reflects the measurement outcome. We can show that this optimal E_{off}^\dagger saturates the thermodynamic bound; in this case, the mutual information generated by the copy is

$$I = p's \ln \left(\frac{s}{f} \right) + p'(1-s) \ln \left(\frac{1-s}{1-f} \right) + (1-p')s \ln \left(\frac{s}{1-f} \right) + (1-p')((1-s) \ln \left(\frac{1-s}{f} \right)). \quad (\text{C14})$$

Using $f = p's + (1-p')(1-s)$,

$$I = (s \ln s + (1-s) \ln(1-s)) - (f \ln f + (1-f) \ln(1-f)). \quad (\text{C15})$$

Comparing Eq. C15 with Eq. C13 shows that $w_T^\dagger = kTI$, and therefore that the protocol with appropriately chosen E_{off}^\dagger reaches the thermodynamic bound for copy cycles if the resultant correlations are not used to extract work.

We note that raising the left well by a negative value of E_{off} to perform decorrelation, in this picture, can only mean raising the right well by $-E_{\text{off}}$ by coupling the system to a reference bit in state 0. An analogous derivation to that presented above holds for this operation, so the result holds for both positive and negative E_{off} . In this analysis, we haven't considered unequal s_R and s_{RL} ; it is not obvious how to adjust this protocol to achieve unequal accuracy.

3. Cause of dissipation in the optimal protocol

As mentioned in the main text, it is actually the decorrelation step that is thermodynamically irreversible, rather than resetting. This is particular clear since the reset energy E_r does not appear in the thermodynamic cost. The cause of irreversibility is the failure to extract work from the combined memory and data bit system as it relaxes from a state more likely to be (memory, data) = (0,0) or (1,1) than (0,1) or (1,0) to one equally likely to be in (0,0), (0,1), (1,0) or (1,1). This is directly analogous to the irreversibility of the free expansion of an ideal gas. A procedure that did extract the maximum work from this decorrelation would be fully reversible, and the overall entropy change of the universe during the cycle would be zero, corresponding to the best possible performance of Maxwell's demon². Reversing the copying procedure using the same data bit, or "uncopying"¹², uses the initial correlation between bits to provide the necessary work to reset the memory bit and is therefore an example of extracting work during decorrelation.

Not only is resetting reversible, it is unnecessary in an optimal cycle. Steps 1 and 2 are the reverse of steps 7 and 8: the initial part of the measurement protocol reverses the reset to the standard state of 0. Thus these steps are unnecessary, and a cycle of steps 3-6 constitutes an equally valid measurement or copy protocol. As the work required for 7 and 8 exactly cancels the work returned by steps 1 and 2, the total work done in this abridged protocol is still given by Eq. C5.

Appendix D: Sampling with unequal accuracies

Supplementary Figure 2 shows that $\eta \leq \frac{1}{2}$ for all p' if $s_R = s_{RL} = s$. In Supplementary Figure 3 (A-C), we plot efficiency η as a function of independently varying s_R and s_{RL} for $p' = 0.5, 0.8, 0.98$. As p' becomes more extreme, a region of $\eta > \frac{1}{2}$ appears and grows, with the maximal value of η found at $s_R \approx 0.5$ and $s_{RL} \approx p'$. Indeed, if we plot η against p' with $s_R = 0.5$ and $s_{RL} = p'$, as in Supplementary Figure 2 (D), we see η approaching unity as $p', s_{RL} \rightarrow 1$. For η to get close to unity, however, requires extreme values of the parameters. We also note that $\eta \rightarrow 1$ does not occur when the dissipation in a phosphorylation-dephosphorylation cycle is low, and is independent of the absolute reaction rates.

In the main text, we gave an intuitive explanation of why an efficiency of 0.5 is limiting in the case $s_R = s_{RL}$, $p' = 0.5$. This was based on considering the heat deposited into the environment (or the total drop in chemical free energy) by the actual transition of the memory bit. A similar analysis applies here, but when $p' \approx s_{RL} \rightarrow 1$ and $s_R \approx 0.5$, the largest contribution to the overall cost comes from copy cycles involving RL rather than R . For the biochemical network, measuring RL involves $s_{RL} - f$ transitions per measurement with a free-energy jump of $E_{s_{RL}}$. For the optimal protocol, the key process is now raising the left well quasistatically from E_{off}^\dagger to $E_{s_{RL}}$, resulting in a transfer of $s_{RL} - f$ particles at an average energy jump of $E_{\text{off}}^\dagger < E < E_{s_{RL}}$. When $p' \approx s_{RL} \rightarrow 1$ and $s_R \approx 0.5$, and unlike the $s_R = s_{RL}$, $p' = 0.5$ case, E_{off} and $E_{s_{RL}}$ are both large and similar in magnitude. This fact means that the deposited heat is close to $E_{s_{RL}}$ and hence the efficiency is close to unity.

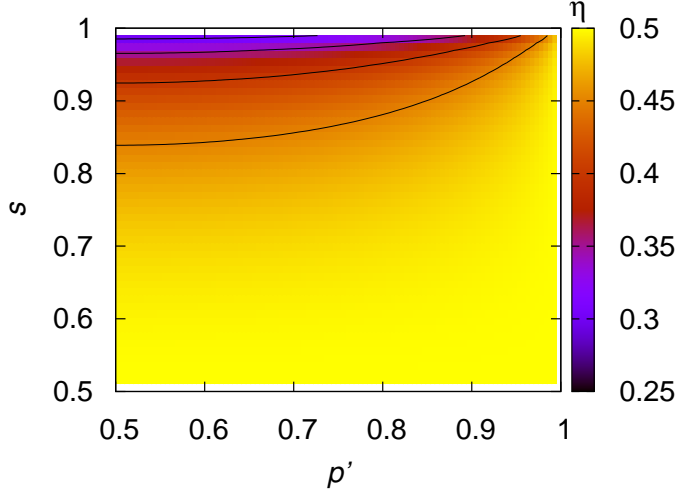


FIG. 7. **Supplementary Figure 2:** Efficiency η as a function of p' and $s = s_R = s_{RL}$. Note that η does not exceed 0.5, and that moving p' away from 0.5 always increases η at fixed s . A mirror image is obtained for $p' < 0.5$.

Appendix E: A clocked biochemical device and protocol

We illustrate a discrete biochemical copy process in Supplementary Figure 4. The readout starts in a state x or x^* determined by the previous measurement. It is then brought into proximity with a receptor (uncorrelated with the previous one) so that catalysis can occur. The readout is allowed to reach a steady state, then removed from the proximity of the receptor.

In this protocol the data and memory are allowed to interact for some period of time and the final result is taken to be the output of a single copy. The receptor state should remain constant in this period (in practice, constitutively active kinases and phosphatases could be used). By contrast, in the cellular network it is most natural to consider a receptor that switches rapidly on timescale of readout modification. Nonetheless, as we show next, provided that receptors are uncorrelated from one measurement to the next and are presented to readouts with the appropriate relative frequency, the cellular and clocked biochemical protocols have the same measurement outcomes and efficiency.

If a series of measurements are performed on uncorrelated receptors using the clocked protocol, the same phosphorylation fraction f as in the cellular network (Eq. 12 of the main text) will be obtained, provided that receptors in the ligand-bound state are present with a probability p' . The accuracy of copies is still given by Eq. 7 of the main text, because s_R and s_{RL} quantify the steady state probabilities of finding x^* when the receptor is in state RL and x when the receptor is in state R , respectively. The work per copy cycle is also given by Eq. 16 of the main text; to see this, note that the free energy of the system changes when the molecule x is converted into x^* or vice versa, either by RL or R ; reactions that overwrite x with x or x^* with x^* do not cost free energy and hence do not contribute to the chemical work. The readout x is converted into x^* by RL with probability $P_{x \rightarrow x^*; RL} = p's_{RL}(1-f)$ and an associated chemical work of $E_{S_{RL}}$. Similarly, $P_{x \rightarrow x^*; R} = (1-p')(1-s_R)(1-f)$, $P_{x^* \rightarrow x; RL} = p'(1-s_{RL})f$, and $P_{x^* \rightarrow x; R} = p's_Rf$, with associated chemical work $-E_{S_R}$, $-E_{S_{RL}}$ and E_{S_R} respectively. Using $f = p's_{RL} + (1-p')(1-s_R)$ and summing gives a dissipation per copy cycle equal to Equation 16 of the main text.

Our clocked biochemical protocol connects to typical computation models that involve manipulating energy landscapes, as illustrated in Supplementary Figure 4 (B). In effect, exposing a readout to a receptor in the RL state immediately biases the landscape towards the x^* “well” and simultaneously lowers the barrier for the transition. Similarly, exposing the readout to R can be interpreted as suddenly raising the x^* “well” and lowering the barrier. The fundamental difference between Supplementary Figure 4 (B) and a optimal computational protocol, such as that in Supplementary Figure 1, is the manner in which the landscape switches suddenly, rather than quasistatically.

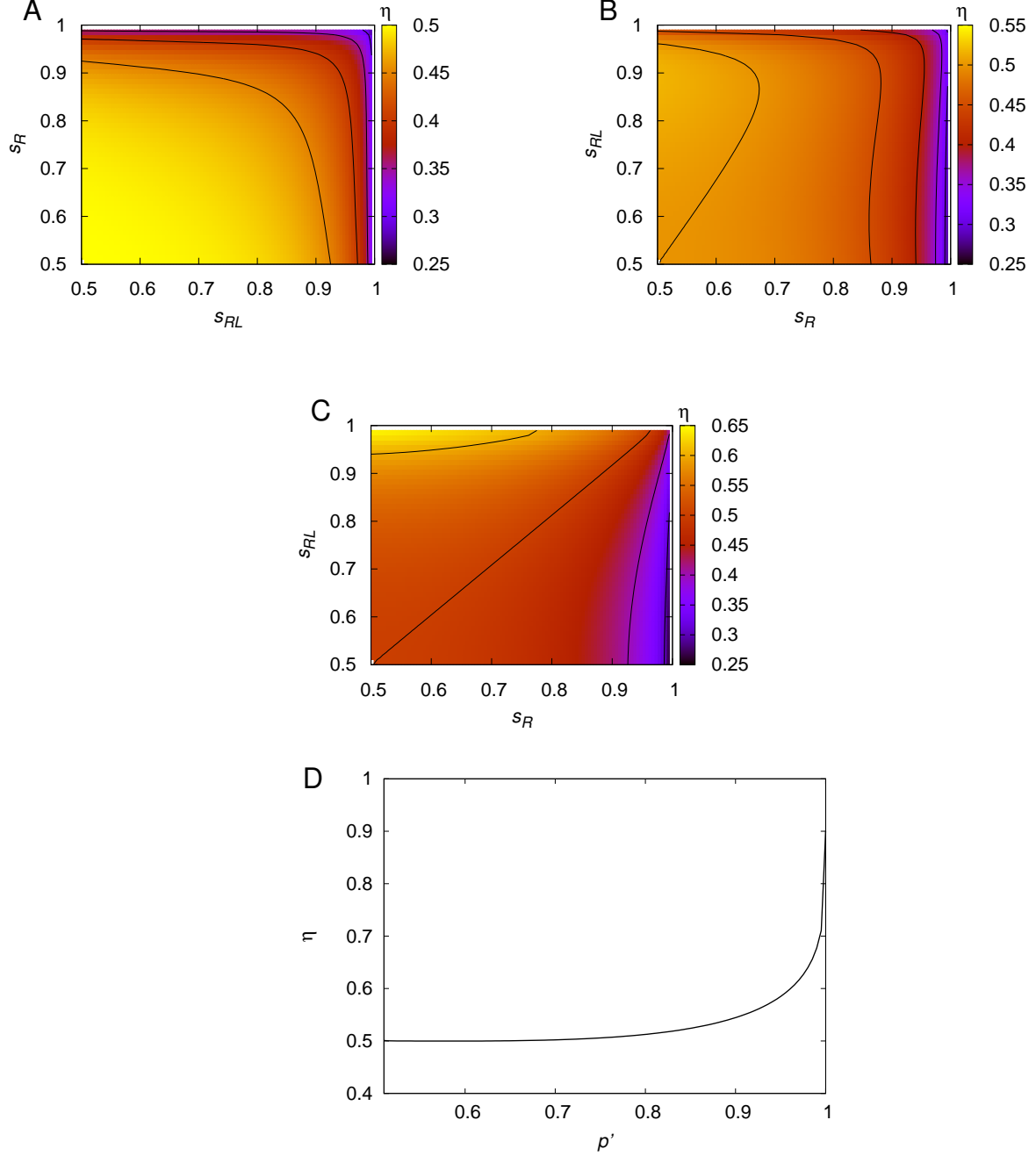


FIG. 8. **Supplementary Figure 3:** Efficiency of the biochemical network η as a function of s_R and s_{RL} for (A) $p' = 0.5$, (B) $p' = 0.8$ and (C) $p' = 0.98$. Note the substantial region in which η exceeds 0.5 that appears as p' grows, centred around $s_{RL} \approx p'$ and $s_R \approx 0.5$. Also note that as $s_{RL} \rightarrow 1$ at fixed p' , η is small. (D) Plot of η against $p' = s_{RL}$ at $s_R = 0.5$. Note that convergence on unity only occurs at extreme values of $s_{RL} = p'$.

Appendix F: A thermodynamically optimal copy operation using biomolecules

1. Detailed calculation for an optimal biochemical bit

The readout begins coupled to a buffer with $\Delta G_p, \Delta G_d = -\Delta G_r$ (ΔG_r assumed to be large and positive, although in fact this initial condition does not influence the copy accuracy or work). There is no receptor in close proximity, but the readout has equilibrated at the end of a previous measurement cycle by a receptor in the R state,

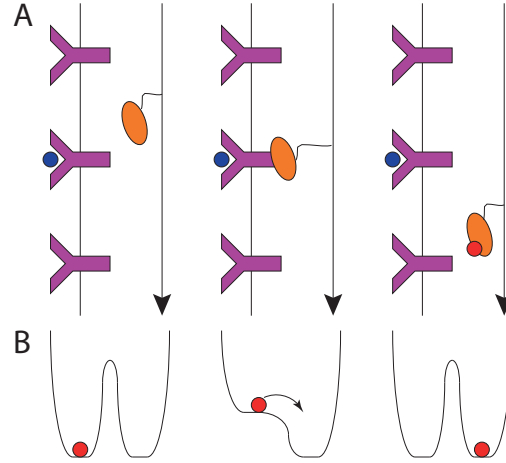


FIG. 9. **Supplementary Figure 4:** An artificial biochemical system in which measurements are performed in a clocked fashion, analogous to computational models. (A) Schematic of the system – the readout, attached to a polymer by a tether, is moved past a series of receptors. (i) The memory is between receptors, and cannot interact with them. (ii) The memory is brought into proximity with a receptor, allowing catalysis and copying. (iii) The memory is moved on, and cannot interact with any receptors. It retains the state of the previous receptor until the next measurement. (B) An interpretation of the process in (A) in a two-state energy landscape picture. In this analogy, the left well corresponds to state x and the right well to x^* . The presence of an enzyme simultaneously lowers the barrier between x and x^* and shifts the equilibrium.

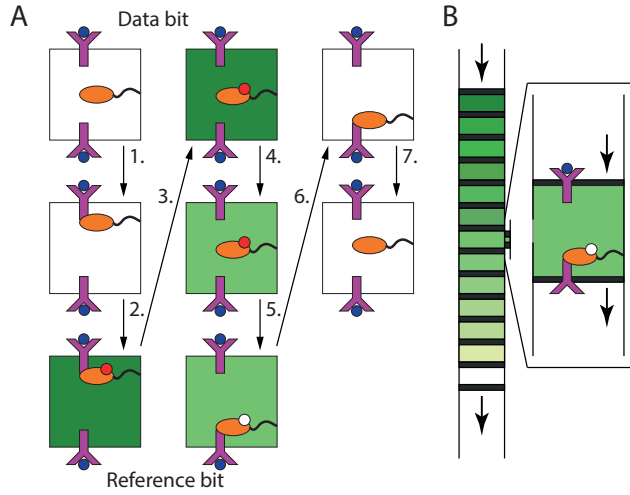


FIG. 10. **Supplementary Figure 5:** A biochemical implementation of an optimal copy device and protocol, in which only the RL state of the receptor is catalytically active. The cycle is illustrated in (A). As in the main text, the system consists of receptors acting as data and reference bits attached to the ends of a reaction volume, and a tethered readout (memory bit). The reference bit is a receptor in state RL , the data bit is a receptor in either R or RL (illustrated here as RL). Initially, the readout is not in close proximity to any receptor, and is in a solution in which $\Delta G_p = \Delta G_s$ is large and positive (the reaction in Eq. G1 is driven to the left), indicated by the light color of the reaction volume. Its is unphosphorylated due to prior coupling to the reference bit. Step 1: the readout is brought into close proximity with the receptor acting as a data bit. Step 2: the solution is quasistatically changed from $\Delta G_p = -\Delta G_s$ to $\Delta G_p = \Delta G_s$ (changed conditions are shown by the darker color). If the receptor is in state RL , the readout tends to be phosphorylated. Step 3: the readout is separated from the receptor acting as a data bit. Step 4: the solution is quasistatically changed to $\Delta G_p = -\Delta G_{off}$, the free energy of reaction at which decorrelation will take place. Step 5: the readout is brought into contact with the receptor acting as a reference bit to allow decorrelation with the data bit. Step 6: the readout is reset by quasistatically changing conditions to $\Delta G_p = \Delta G_s$. Step 7: the readout is separated from the reference bit, restoring the initial state. (B) A device for implementing this cycle. A small reaction volume is coupled to a series of reservoirs of varying ATP, ADP and P content. The current reservoir can be changed by pushing a piston. Similarly, the receptors and readout can be brought in an out of proximity by manipulation of a second piston.

and therefore is in state x with probability $1/(1 + \exp(-\Delta G_r/kT))$.

1. The readout is brought into close proximity with a receptor of known state R ; no reactions take place on average.
2. $\Delta G_p, \Delta G_d$ are slowly (quasistatically) raised from $-\Delta G_r$ to 0. The chemical work is given by the average number of reactions of a given type, multiplied by the associated chemical work, integrated over the whole process. In the presence of a receptor in state R , only $R + x^* \rightleftharpoons R + x + P$ is possible, and in an infinitesimal step from ΔG_d to $\Delta G_d + d\Delta G_d$, the average number of net dephosphorylation events is

$$n_{\text{dephos}} = \frac{\exp(-\Delta G_d/kT)}{1 + \exp(-\Delta G_d/kT)} - \frac{\exp(-(\Delta G_d + d\Delta G_d)/kT)}{1 + \exp(-(\Delta G_d + d\Delta G_d)/kT)} = -\frac{\exp(-\Delta G_d/kT)}{(1 + \exp(-\Delta G_d/kT))^2} \frac{d\Delta G_d}{kT}. \quad (\text{F1})$$

Thus

$$w_{2,\text{chem}} = \int_{-\Delta G_r}^0 \frac{d\Delta G_d}{kT} \frac{(\Delta G_d + \Delta G_{x/x^*}) \exp(-\Delta G_d/kT)}{(1 + \exp(-\Delta G_d/kT))^2}, \quad (\text{F2})$$

since $-(\Delta G_d + \Delta G_{x/x^*})$ is the chemical work done by the buffer in a single dephosphorylation reaction catalysed by R . Computing the integral,

$$w_{2,\text{chem}} = -kT \ln \left(\frac{2}{1 + \exp(-\Delta G_r/kT)} \right) + \frac{\Delta G_r \exp(-\Delta G_r/kT)}{1 + \exp(-\Delta G_r/kT)} - \Delta G_{x/x^*} \left(\frac{1}{2} - \frac{1}{1 + \exp(-\Delta G_r/kT)} \right). \quad (\text{F3})$$

3. The readout is brought into close proximity with a receptor of unknown state (ligand-bound with probability p'). $\Delta G_p, \Delta G_d$ are then slowly lowered to $-\Delta G_s$. In this step, the state of the readout is set to match that of the receptor (with some error). Proceeding analogously to Step 2, and considering the possibility of the receptor being either R or RL with probabilities $1 - p'$ and p' , respectively,

$$w_{3,\text{chem}} = +kT \ln \left(\frac{2}{1 + \exp(-\Delta G_s/kT)} \right) - \frac{\Delta G_s \exp(-\Delta G_s/kT)}{1 + \exp(-\Delta G_s/kT)} + (1 - 2p') \Delta G_{x/x^*} \left(\frac{1}{2} - \frac{1}{1 + \exp(-\Delta G_s/kT)} \right). \quad (\text{F4})$$

4. The readout is removed from close proximity with the receptor. No reactions occur on average.
5. $\Delta G_p, \Delta G_d$ are set to ΔG_{off} . No reactions occur on average. This stage constitutes the end of the copy; if the unknown receptor is in state RL , then the readout is in x^* with probability $s = 1/(1 + \exp(-\Delta G_s/kT))$. Similarly, if the unknown receptor is in state R , the readout is in x with probability $s = 1/(1 + \exp(-\Delta G_s/kT))$. Thus the protocol performs a copy of accuracy s .
6. We now decorrelate the memory and data bits. The readout is brought into close proximity with a known receptor of state R . The readout relaxes to a state reflective of ΔG_{off} via the reaction $R + x^* \rightleftharpoons R + x + P$. The chemical work done is

$$w_{6,\text{chem}} = -(\Delta G_{\text{off}} + \Delta G_{x/x^*}) \times p' \left(\frac{1}{1 + \exp(-\Delta G_s/kT)} - \frac{1}{1 + \exp(-\Delta G_{\text{off}}/kT)} \right) + (\Delta G_{\text{off}} + \Delta G_{x/x^*}) \times (1 - p') \left(\frac{1}{1 + \exp(-\Delta G_s/kT)} + \frac{1}{1 + \exp(-\Delta G_{\text{off}}/kT)} - 1 \right). \quad (\text{F5})$$

7. The readout molecule is reset by quasistatically lowering $\Delta G_p, \Delta G_d$ to $-\Delta G_r$ from ΔG_{off} , returning it to a state dominated by x .

$$w_{7,\text{chem}} = +kT \ln \left(\frac{1 + \exp(\Delta G_{\text{off}}/kT)}{1 + \exp(-\Delta G_r/kT)} \right) - \frac{\Delta G_r \exp(-\Delta G_r/kT)}{1 + \exp(-\Delta G_r/kT)} - \frac{\Delta G_{\text{off}} \exp(\Delta G_{\text{off}}/kT)}{1 + \exp(\Delta G_{\text{off}}/kT)} + \Delta G_{x/x^*} \left(1 - \frac{1}{1 + \exp(-\Delta G_{\text{off}}/kT)} - \frac{1}{1 + \exp(-\Delta G_r/kT)} \right). \quad (\text{F6})$$

8. The readout molecule is separated from the known receptor. No reactions occur on average. The system has now been returned to the initial state.

Summing Eqs. F3, F4, F5 and F6 gives a total chemical work for the cycle of

$$w_{\text{chem}} = kT \ln \left(\frac{1 + \exp(\Delta G_{\text{off}}/kT)}{1 + \exp(-\Delta G_s/kT)} \right) - \frac{\Delta G_s \exp(-\Delta G_s/kT)}{1 + \exp(-\Delta G_s/kT)} - \Delta G_{\text{off}} \frac{p' + (1 - p') \exp(-\Delta G_s/kT)}{1 + \exp(-\Delta G_s/kT)}. \quad (\text{F7})$$

Using the fact that the probability of the copy resulting in x^* (at the end of step 5) is $f = p's + (1 - p')(1 - s)$, the fact that the accuracy s is given by $s = 1/(1 + \exp(-\Delta G_s/kT))$, and the identity $\exp(z) \equiv (1 + \exp(z))/(1 + \exp(-z))$,

$$w_{\text{chem}} = kT \ln \left(\frac{1 + \exp(-\Delta G_{\text{off}}/kT)}{1 + \exp(-\Delta G_s/kT)} \right) - (1 - s)\Delta G_s + (1 - f)\Delta G_{\text{off}}. \quad (\text{F8})$$

Similarly to Supplementary Discussion 3, we can minimize the work with respect to ΔG_{off} at fixed p' , s and f , obtaining $\Delta G_{\text{off}}^\dagger = kT \ln(f/(1 - f))$. Substituting for $\Delta G_{\text{off}}^\dagger$ and ΔG_s using f and s , we see that this particular protocol involves work

$$w_{\text{chem}} = kT (s \ln s + (1 - s) \ln(1 - s) - f \ln f - (1 - f) \ln(1 - f)), \quad (\text{F9})$$

which is identical to the information gained by the measurement of the data (Supplementary Eq. C15). Thus the biochemical protocol with decorrelation free energy $\Delta G_{\text{off}}^\dagger = kT \ln(f/(1 - f))$ is a thermodynamically optimal protocol.

2. Subtleties in the comparison between biochemical systems and energy landscapes

a. The role of receptors

In the energy-landscape description presented in Supplementary Figure 1, it was assumed that we are separately able to lower the barrier between wells and raise one well in energy with respect to the other. In the quasistatic biochemical protocol presented in the main text, the receptor acts as a catalyst (lowering the barrier between activation states of the readout), but the state of the receptor also determines which state is favourable. Thus it is not possible to formally separate biasing and lowering/raising of the barrier in the same way as in the energy landscape picture (the strength of the bias when a receptor is present, but not its direction, is determined by the buffer to which the memory is connected). Indeed, it is not really meaningful to draw energy landscapes in a two-state description of the biochemical system in which the fuel is coarse-grained away, unless there is a single receptor present. As we demonstrate, however, this does not prevent the biochemical system performing efficient measurement, and the purpose of each of the 8 steps in the biochemical protocol is closely analogous to its counterpart in Supplementary Figure 1.

b. Chemical work

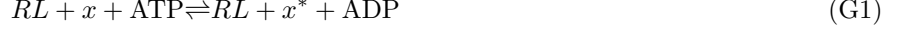
We claim that there is a close analogy between the optimal biochemical protocol in the main text and the energy-landscapes description in Supplementary Figure 1. Further, we claim that the purpose of the individual steps are the same. However, the work calculated for the individual steps are quite different; for example, the “chemical work” during the decorrelation step (step 6) in the biochemical protocol is non-zero, whereas the work done is zero in the energy landscapes picture.

The work for the protocol in Supplementary Figure 1 is calculated in Supplementary Discussion 3 as is typical in stochastic thermodynamics⁴⁵. Work is done when the energy landscape is manipulated, and heat is exchanged when the particle moves within the landscape. Although this approach is well-established for such systems, it is less clear how to proceed when the external manipulation involves the concentrations of reactants, as in our biochemical approach. Furthermore, as discussed above, the use of (free-) energy landscapes to describe the biochemical system at a coarse-grained level is not straight-forward.

Instead, we choose to calculate the change in chemical free energy associated with the buffers (the negative of the “chemical work” they perform). This quantity is well defined, and in a measurement cycle (in which the memory returns to its initial state) corresponds to the overall change in free energy of the entire system. A decrease in free energy of the system corresponds to a reduction of its ability to do work, and is therefore “dissipation” unless this drop is harnessed to do work.

Appendix G: An optimal protocol involving a receptor that functions only as a kinase

It is possible to construct a measuring device using only the reaction



if the R state of the receptor does not catalyse a reaction. The procedure is illustrated in Supplementary Fig. 5, and outlined in detail below. As in Supplementary Discussion 6, we calculate the chemical work performed by the ATP/ADP reservoirs during a cycle, in which the unknown receptor is in state RL with probability p' . We start with the readout isolated from any receptors, and in a buffer with a high ADP concentration and a low ATP concentration. In this case, the reaction in Eq. G1 is driven to the left; $\Delta G_p = \Delta G_s$ where ΔG_s is large and positive. The readout has previously been equilibrated by a receptor in the RL state at this value of ΔG_p ; it is therefore predominantly in the x state. Note that since the measurement of R will be passive, the initial state determines the accuracy of measurement and hence ΔG_s appears here, rather than an arbitrary reset accuracy ΔG_r .

1. The readout is brought into close proximity with the unknown receptor. No reactions occur on average
2. ΔG_p is slowly (quasistatically) lowered from ΔG_s to $-\Delta G_s$. If the unknown receptor is in state RL , the readout tends to be converted to x^* – no reactions take place if the receptor is in state R . The average chemical work done is

$$\begin{aligned} w_{2,\text{chem}} &= p' \int_{\Delta G_s}^{-\Delta G_s} \frac{d\Delta G_p}{kT} \frac{(\Delta G_p - \Delta G_{x/x^*}) \exp(-\Delta G_p/kT)}{(1 + \exp(-\Delta G_p/kT))^2}, \\ &= p' \Delta G_{x/x^*} \left(\frac{1}{1 + \exp(-\Delta G_s/kT)} - \frac{1}{1 + \exp(\Delta G_s/kT)} \right). \end{aligned} \quad (G2)$$

The relation $\exp(x) \equiv (1 + \exp(x))/(1 + \exp(-x))$ is useful in deriving this result.

3. The readout is separated from the receptor; no reactions take place on average.
4. The buffers are slowly changed so that $\Delta G_p = -\Delta G_{\text{off}}$. No reactions take place. This stage constitutes the end of the copy; if the unknown receptor is in state RL , then the readout is in x^* with probability $s = 1/(1 + \exp(-\Delta G_s/kT))$. Similarly, if the unknown receptor is in state R , the readout is in x with probability $s = 1/(1 + \exp(-\Delta G_s/kT))$. Thus the copy has been performed with accuracy $s = 1/(1 + \exp(-\Delta G_s/kT))$.
5. The following steps involve decorrelation and resetting. The readout is brought into contact with the receptor of known state RL . The readout relaxes to a state representative of the free-energy difference $\Delta G_p = -\Delta G_{\text{off}}$. The chemical work done is

$$\begin{aligned} w_{5,\text{chem}} &= p' (\Delta G_{x,x^*} + \Delta G_{\text{off}}) \left(\frac{1}{1 + \exp(-\Delta G_{\text{off}}/kT)} - \frac{1}{1 + \exp(-\Delta G_s/kT)} \right) \\ &\quad + (1 - p') (\Delta G_{x,x^*} + \Delta G_{\text{off}}) \left(\frac{1}{1 + \exp(-\Delta G_{\text{off}}/kT)} - \frac{1}{1 + \exp(\Delta G_s/kT)} \right). \end{aligned} \quad (G3)$$

6. The buffer is slowly changed from $\Delta G_p = -\Delta G_{\text{off}}$ to $\Delta G_p = \Delta G_s$. The readout is restored to a state dominated by x . The chemical work done is

$$\begin{aligned} w_{6,\text{chem}} &= \int_{-\Delta G_{\text{off}}}^{\Delta G_s} \frac{d\Delta G_p}{kT} \frac{(\Delta G_p - \Delta G_{x/x^*}) \exp(-\Delta G_p/kT)}{(1 + \exp(-\Delta G_p/kT))^2} = kT \ln \left(\frac{1 + \exp(-\Delta G_{\text{off}}/kT)}{1 + \exp(\Delta G_s/kT)} \right) \\ &\quad + \frac{\Delta G_s \exp(\Delta G_s/kT)}{1 + \exp(\Delta G_s/kT)} + \frac{\Delta G_{\text{off}} \exp(-\Delta G_{\text{off}}/kT)}{1 + \exp(-\Delta G_{\text{off}}/kT)} + \Delta G_{x/x^*} \left(\frac{1}{1 + \exp(\Delta G_s/kT)} - \frac{1}{1 + \exp(-\Delta G_{\text{off}}/kT)} \right). \end{aligned} \quad (G4)$$

7. The readout is removed from the receptor. No reactions take place. The system is restored to the initial state.

Summing over all terms gives

$$w_{\text{chem}} = kT \ln \left(\frac{1 + \exp(-\Delta G_{\text{off}}/kT)}{1 + \exp(\Delta G_s/kT)} \right) + \frac{\Delta G_s \exp(\Delta G_s/kT)}{1 + \exp(\Delta G_s/kT)} + \Delta G_{\text{off}} \frac{(1 - p') + p' \exp(-\Delta G_s/kT)}{1 + \exp(-\Delta G_s/kT)}. \quad (G5)$$

Utilising $\exp(x) \equiv (1 + \exp(x))/(1 + \exp(-x))$ once more, The Eq. G5 can be re-written

$$w_{\text{chem}} = kT \ln \left(\frac{1 + \exp(\Delta G_{\text{off}}/kT)}{1 + \exp(-\Delta G_s/kT)} \right) - \frac{\Delta G_s \exp(-\Delta G_s/kT)}{1 + \exp(-\Delta G_s/kT)} - \Delta G_{\text{off}} \frac{p' + (1 - p') \exp(-\Delta G_s/kT)}{1 + \exp(-\Delta G_s/kT)}, \quad (G6)$$

which is identical to Supplementary Eq. F7. The above method therefore has the same outcome and thermodynamic cost as those analysed in Supplementary Discussions 3 and 6. It has the advantage of requiring the manipulation of ΔG_p only, but the disadvantage that the reset step is actually necessary. The reset step is needed because the R state does not actively set the memory to x ; we rely on the memory being prepared in the x state prior to copy.
